Establishing a multicellular model by three-dimensional cell-assembly technique for metabolic syndrome

Mingen Xu[1,2,3], Yongnian Yan[1,2], Haixia Liu[1,2], Ri Yao[1,2], and Xiaohong Wang[1,2]*

1 Key laboratory for Advanced Materials Processing technology, Ministry of Education & Center of Organ Manufacturing, Department of mechanical Engineering, Tsinghua University, Beijing 100084, P.R. China

2 Institute of Life Science & Medicine, Tsinghua University, Beijing 100084, P.R. China

3 Center Laboratory of Tissue Engineering, Hang Zhou Dianzi University, 310018, P.R. China

Correspondence should be addressed to W.X.H (wangxiaohong@tsinghua.edu.cn) or X.M.E (xumingen@tsinghua.edu.cn)

Phone: 86-10-62773202; Fax: 86-10-62783565

Abstract

One of the major obstacles in developing multifunctional drugs for the metabolic syndrome (MS) is lack of *in vitro* models that capture more complex features of the disease. Here we give the first report that establishes an energy metabolic system model using cell-assembly technique which can assemble cells into designated places to form complex three-dimensional structures. Adipose-derived stromal cells were assembled and induced differentiation into adipocytes and endothelial cells; pancreatic islets were then deposited at designated locations and constituted adipoinsular axis with adipocytes. Analysis of the factors involved in energy metabolism showed our system could capture more physiological and pathophysiological features of the *in vivo* energy metabolism. Drugs known to have effects on MS showed accordant effects in the systems. Construction and study of such multicellular systems could help us better understand pathogenesis of MS, develop new technologies for drug discovery, and foster applications in tissue engineering and metabolomics profiling.

Researchers have recently developed techniques to fabricate tissues and organs in which both cells and biomaterials have carefully defined architectures. Three-dimensional (3-D) bioassembly tool is capable of extruding cells and biomaterials into spatially organized, 3-D constructs [1]. Cell printing equipments can print cells as a stream of drops in 3-D positions that mimic their respective positions in organs [2,3]. We have recently developed a 3-D cell-assembly technique

based on Rapid Prototyping (RP) [4,5]. This technique can put different cells and materials into designated places to form complex 3-D structures. The designed architecture facilitates cell growth, organization and differentiation. Hepatocytes have been assembled with gelatin hydrogel to build 3-D structures, in which the viabilities and functions of the cells could remain more than 60 days [6].

Tissue engineering endeavored to manufacture tissues and organs, but pay little attention to establish physiological system models[7,8]. However, in study of complex physiological processes, there is an increasing demand for *in vitro* 3-D models that can capture more of the relevant complexity than what traditional two-dimensional (2-D) cultures achieve [9-11]. In the field of drug discovery, high-throughput screening is ineffective due to its failure in capturing complex pathological features *in vivo* environment [12,13]. More recently, some *in vitro* 3-D models have been applied in research pattern formation[14], tumor growth[15] and apoptosis[16], but limited to study of simple physiologic processes by slow spontaneous aggregation of spheroids with poorly controlled structure.

Metabolic syndrome (MS) is a cluster of growing epidemic diseases including obesity, diabetes, hypertension, and atherosclerosis[17,18]. Recently, the pharmaceutical industry has shown great interest in developing drugs that can target MS as a whole [19]. Researchers including ourselves have devoted to find out drug targets and establish models for MS[20-23]. However, there are still no approved drugs that can reliably reduce all of the metabolic risk factors over the long term. One of the major obstacles is the lack of *in vitro* models that can capture more pathological features of MS. MS is largely presented as energy metabolic turbulence and cardiovascular disease (CVD); adipocytes and β-cells usually constitute adipoinsular axis to regulate energy metabolism[24]; and endothelial cell dysfunction can connect the pathogenesis of energy metabolic turbulence with CVD[25]. With these mechanisms in mind we attempt to organize the related cells to establish MS models.

Here we report the feasibility of constructing an *in vitro* multicellular 3-D model of energy metabolic system for MS, using our cell-assembly technique. Adipose-derived stromal (ADS) cells[26,27] were assembled in a well designated 3-D structure and were controlled differentiation into adipocytes and endothelial cells based on their respective positions within the structure; pancreatic islets were then deposited at designated micro-holes. We also tested the factors

involved in energy metabolism and endothelial dysfunction of the multicellular model, tested whether chronic exposure to high glucose, a major inducement of MS, could lead to similar pathological changes of the multicellular model **to** MS, and tested whether drugs known to have effects on MS manifest accordant effects in the multicellular system.

RESULTS

Assembling of 3-D multicellular system

Considering the important roles of adipocytes, β-cells and endothelial cells in energy metabolism and MS pathogenesis, we assumed that these types of cell would be required for construction of model for MS. We selected ADS cells isolated from rat, which can differentiate into adipocytes and endothelial cells. After several comparative experiments about biocompatible materials, we mixed ADS cells with gelatin, alginate and fibrinogen solutions sequentially. A software package was employed to fabricate the complex structure model with orderly channels (**Fig. 1 a**). Following the designed model, a nozzle controlled by computer was used to deposit the mixture on a glass chip at a temperature of 10 ℃ (gelatin at gel state) and generate 3-D structures (**Fig. 1 b**). Then, alginate was crosslinked with $CaCL_2$ and the fibrinogen with thrombin. Once the mixture was crosslinked, the whole construct could be handled easily without losing its integrity; cells were homogeneous embedded in the matrices **(Fig. 1c, d)**, and the hydrogel state could remain at least 8 weeks. The complete process required only ~20 min. Scanning electron micrographs showed the development of extensive extracellular matrix (ECM) and cell networks in the structure after 6 days of culture **(Fig. 1d**). The pancreatic islets (contain β-cells) from rat were deposited to designated micro holes in the 3-D structure at the 7^{th} d. Anti-insulin immunostaining showed that 90% of the pancreatic islets could keep their integrity of globoid shape more than three weeks in the structure (**Fig. 1e**). Some envelopes of islet were broken, but the β-cells still congregated and kept secreting insulin. (**Fig. 1f**).

To test whether ADS cells in the 3-D structure can be controlled differentiate into endothelial cells and adipocytes, we examined composition and distribution of the cells in the 3-D structure by immunostaining and Oil Red O staining. After 3 days of culture with endothelial growth factor (EGF), CD34 (ADS cells and endothelial cells indicator) and CD31 (mature endothelial cells indicator) staining revealed that over 90% of ADS cells on the walls of the channels were differentiated into mature endothelial cells (CD31+/CD34+) and connected with each other

forming vessel-like structure. (**Fig. 2a, c, e, f**). This differentiation of ADS cells was based on EGF inducing (Fig2 b, d) and cell position in the 3-D structure (**Fig. 2e, f**). From the 4th day, the structures were treated with insulin, IBMX and dexamethasone for 3 d. At the 12th day, Oil red O staining revealed that ADS cells in the structure differentiated into adipocytes with a spherical shape (**Fig. 2g**). The cells under the walls of the channels were more sensitive to differentiation into adipocytes than those on the surface of the walls. However, if not induced with EGF, more than 90% of cells on the walls of channels would differentiate into adipocytes (**Fig. 2h**).

Dynamic insulin secretion

To determine whether β-cells assembled in the system can mimic *in vivo* function, we used a perfusion system for a time-dependent estimation of insulin response to glucose stimulation. **Figure 3** shows the dynamic insulin release patterns of free or assembled β-cells stimulated by glucose. In response to 15 mM glucose stimulation, assembled β-cells showed a significant increase in insulin secretion compared to free β-cells. To determine whether chronic exposure to high glucose could cause pathological changes of the β-cells, we culture free or assembled β-cells with high-glucose (15 mM). After 5 days of culture, both free β-cells and assembled β-cells showed dramatic decreases in glucose-induced insulin release, and the decrease rate of the assembled β-cells was higher than that of the free β-cells. Nateglinide could revise the insulin secretion decrease of the assembled and free β-cells; whereas rosiglitazone only had the same effects on the assembled β-cells.

Notably, after pre-cultured with high glucose, the glucose-induced insulin secretion peak of the assembled β-cells was delayed compared to normal control, this delay could be revised by nateglinide, however, this phenomenon was not observed in the free β-cells. Derangements in the kinetics of insulin release, including the decrease and delay of the secretion peak value, were one of main characteristics of diabetes[28,29]. These results are consistent with the other *in vivo* experiments[30,31], suggesting that the adipocytes in the 3-D structure could help the β-cells to capture more pathologic feature of MS. Further investigation of adipocytokine secretion would subsequently reveal the mechanism of this phenomenon.

Glucose consumption, FFA release, and Adipogenesis

Glucose consumption and free fatty acids (FFA) mobilization of adipocytes are two basic metabolic processes in energy metabolism. To determine the glucose consumption of cells in the

2-D, 3-D (without β-cells) and multicellular 3-D (with β-cells) culture systems, we culture the cells with 25 mM glucose, and thereafter the media were collected for glucose consumption assays (**Fig. 4a**). Cells in the 3-D structure showed higher glucose consumption than in the 2-D structure, seeding β-cells in the 3-D structure significantly enhanced the glucose consumption. Similarly, after stimulated with isoproterenol, cells in the 3-D structure showed higher FFA release than in the 2-D structure, and the β-cells significantly increase the FFA release of the adipocytes (**Fig. 4b**).

To determine whether long-term exposure to high glucose could cause similar pathological changes of glucose and lipid metabolism of MS, we cultured cells with high-glucose (15mM) for 7 d. Pre-culture with high glucose inhibited the glucose consumption of all culture systems, the decrease rates of the multicellular 3-D system was the highest. Rosiglitazone revised the glucose consumption inhibited by high glucose, the increase rates of the multicellular 3-D system was the highest. Contrarily, pre-culture with high glucose increased the isoproterenol-induced FFA release of all culture systems. Rosiglitazone just inhibited the FFA release which increase in the multicellular 3-D system. These results suggest that β-cells assembled in the structure facilitate the system to mimic glucose and FFA metabolism dysfunction of MS and to show more obvious effects of rosiglitazone.

Synthesize and storage fatty acid with overnutrition is the main function of adipocytes and also the pathogenesis of obesity. To test whether high glucose promotes adipogenesis of adipocytes in different culture systems, we cultured cells with high glucose. After total of 12 days of culture, the adipogenesis of the 2-D, 3-D and multicellular 3-D system were increased by 2.1, 5, and 7.3 folds compared to normal level, respectively (**Fig 4c**). Rosiglitazone could increase the adipogenesis of all the groups; the increase rate of the multicellular 3-D culture system was the lowest. These results suggest that, in the multicellular 3-D system, the assembled β-cells promote adipogenesis of adipocytes, but rosiglitazone has only moderate effect on adipogenesis. These results accord with the other *in vitro* researches[32,33].

Adipocytokine

In addition to the storage of lipid, adipocytes perform an endocrine function by secreting adipocytokines to regulate energy metabolism[34]. To study the adipocytokine secreted by

adipocytes, we analyzed the secretion of leptin, resistin, and adiponectin of different culture systems. Leptin can inhibit both energy intake and insulin secretion, and is antagonistic to insulin action. Leptin secretion of adipocytes in the 3-D structure was higher than that in the 2-D structure; β-cells inhibit leptin secretion of adipocytes in the 3-D structure (**Fig. 5a**). Resistin is capable of being antagonistic to insulin action and, thus, may serve as a link between obesity and type 2 diabetes. Adipocytes in the 3-D structure showed higher resistin secretion than in the 2-D structure (**Fig. 5b**). Adiponectin can increase insulin sensitivity and protect endothelial cells. Adipocytes in 3-D structure showed higher adiponectin secretion than in 2-D culture (**Fig. 5c**). These data suggest that adipocytes in the 3-D culture systems have higher adipocytokine secretion than in the 2-D culture system. However β-cells have no obvious effect on normal secretion level of adiponectin and resistin, except leptin.

To determine whether chronic exposure to high glucose can induce pathological changes of adipocytokine secretion of adipocytes, we cultured the different systems with high glucose. Compared with the normal secretion level, pre-culture with high glucose: (i) increased the leptin secretion of all groups; (ii) increased the resistin secretion of all groups; (iii) inhibited the adiponectin secretion of all groups; (iv) adipocytokine secretion changes in the multicellular 3-D group were more moderate than those in the other groups. Rosiglitazone could restore the leptin, resistin, and adiponectin secretion derangement; these effects were more obvious in the multicellular 3-D group. These results are consistent with the other *in vivo* experiments[35,36].

Endothelial dysfunction

Nitric oxide (NO) and endothelin-1 secretion derangements have been identified as major contributors to endothelial dysfunction associated with MS [25]. To study the NO and endothelin-1 secretion of endothelial, we cultured different systems with high glucose for two days. After stimulated with high glucose, endothelial cells in the 3-D structure showed higher endothelin-1 secretion rate than in the 2-D culture, and the assembled β-cells increased the endothelin-1 secretion rate of endothelial in the 3-D structure; Rosiglitazone decreased the endothelin-1 secretion stimulated by high glucose; the decrease rate of the multicellular 3-D system was the highest (**Fig. 6a**). However, we did not find any obvious modification of NO production in the 2-D and 3-D systems after stimulating with high glucose, except for the increase of the

multicellular 3-D system. Rosiglitazone could significantly increase the NO production of the 3-D and multicellular 3-D systems, but has no effect on the 2-D system (**Fig. 6b**).

Our results suggest that the secretion of β-cells could stimulate the secretions of endothelin-1 and NO. Insulin plays an important role in inducing endothelin-1 and NO release; Anti-insulin could decrease the ET-1 and NO secretion of the multicellular system, but has no significant effects on other systems without β-cells. These results suggest that β-cells increase ET-1 and NO secretion of culture system largely through secretion insulin, comparing with other culture systems, endothelial cells in the multicellular 3-D system could capture more pathological features of MS and rosiglitazone had more accordant effects on these systems[37,38].

DISCUSSION

We here give the first description to the establishment of energy metabolic system model with cell-assembly technique. This approach integrates recent advances of tissue engineering, stem cell and MS into more efficient and wildly useful methodology. Previous researches demonstrated that, in comparison with conventional 2-D cultures, cells in 3-D cultures more closely resemble to the *in vivo* situation with regards to cellular environment, cell shape, gene expression and biological behavior[39,40]. Here we used the cell-assembly technique to design and assemble a complex architecture with internal channels, which based on the requirements of growth, function, differentiation, signaling of different types of cells, as well as different detecting technologies. Results showed that cells in the 3-D structure have higher bioactive viabilities than in the 2-D culture system, including insulin secretion, glucose and lipid metabolism, adipocytokine secretion, NO and endothelin-1 secretion. These results demonstrated that the well-designed 3-D architecture could provide the different types of cells with suitable environment that facilitates cells keeping their respective bioactivities and functions. For example, adipocytes in our 3-D structures could capture distribution, morphology and bio-behavior features which ordinarily appear *in vivo* environment. These results are consistent with the recent researches of 3-D cultivation of preadipocytes on Fibrous Polymer Scaffolds[41].

ADS cells are multipotent cells found in adipose tissue and have received more attentions recently[42]. This is the first attempt that ADS cells were controlled differentiation into different targeted cell types according to their positions within an orderly 3-D structure. Immunostaining tests have demonstrated that EGF could easily induce ADS cells on the walls of the channels to

differentiate into mature endothelial cells and form tubular structures throughout the engineered 3-D structures. Contrarily, after pre-culture with EGF, ADS cells under the walls of the channels were more sensitive to differentiation into adipocytes than the cells on the walls. The reasons could be explained as: (i) the EGF concentration under the walls of the channels was lower than that on the surface of the channels due to the diffusion gradient; (ii) the mechanical properties of the surface of the channels could induce the ADS cells to differentiate into endothelial cells more easily; (iii) once differentiated into mature endothelial cells, the ADS cells will lost other differentiation potentials. Further investigations were needed to confirm these hypotheses. At present, one of the major obstacles in engineering thick and complex tissues is the need to vascularize the tissue *in vitro* for maintaining cell viability during tissue growth and inducing structural organization[43]. Our technique has therefore provided a new approach to engineer orderly endothelial vessel networks *in vitro*.

We organized ADS cells, endothelial cells, adipocytes and β-cell in an orderly 3-D structure and mimicked their respective *in vivo* positions. We hypothesized that these cells could mimic energy metabolic system through paracrine and intercellular interactions as that *in vivo*. The results demonstrate that adipocytes in the system could influence the glucose-induced insulin secretion kinetics of the β-cells. After long-term exposure to high glucose, adipocytes became obese and secreted more FFA, leptin and resistin, which were actively involved in crosstalk with β-cell, decreased and delayed the insulin secretion peak value of β-cell[44]. Moreover, secretions of β-cells also affect the functions of adipocytes, such as increasing glucose consumption, FFA release and adipogenesis, decreasing leptin release, and increasing homeostasis of adipocytokines secretion to high glucose stimulation. Endothelial cells formed vessel wall-like structure on the walls of channels and then constructed an endothelial barrier between adipocytes and β-cells as that *in vivo*. In summary, adipocytes and β-cell of the multicellular system constituted adipoinsular axis to regulate energy metabolism, secretions from adipocytes and β-cells affected the ET-1 and NO release of endothelial cells, all these intercellular interactions are coincidence with those of *in vivo* experiments[45,46]. Notably, the major inducement of MS, chronic exposure to high glucose, causes more similar pathological changes of MS in the multicellular system, including obesity, insulin and adipocytokines secretion derangement, insulin resistance, and endothelial cells dysfunction. Moreover, drugs that have known effects on MS have shown accordant effects in the

system[47].

Establishment of such a multicellular 3-D model of energy metabolic system has broadly practical and scientific implications. This model provides the essential steps in pathogenesis study and drug discovery of MS *in vitro*. As MS is a cluster of diseases, this model can also be used in drug discovery for obesity, diabetes, hypertension, dyslipidemia, atherosclerosis, respectively. We organized these different types of cells in a well-defined geometry, which is compatible with *in situ* assays via standard and confocal microscopy (for example, with nondestructive fluorescent probes, immunolabels), biosensor array, as well as bulk assays of cell secretion and gene expression. Considering the technique is automatic, versatile, rapid, and high-throughput productive, it has potential applications in high-content drug screening technology. Moreover, if we assemble cells that isolated from human beings, this 3-D model can capture species specific facets in drug discovery. Additionally, construction and study of such multicellular 3-D system can not only provide research model for studying the cell-cell interaction, stem cell differentiation, and cell organization mechanism, but also provide new approaches for tissue engineering (especially for vascularization). This new 3-D system closely mimics the *in vivo* energy metabolic features, so it has potential applications in metabolomics profiling.

METHODS

Cell culture ADS cells were isolated from rat subcutaneous adipose tissues[26]. The epididymal adipose tissues from Sprague-Dawley rats (100~150 g, Beijing university medica Center of Laboratory Animals) were excised, washed sequentially in serial dilutions of betadine and finely minced in PBS. Tissues were digested with 0.075% Type II collagenase (sigma) at 37℃ for 30 min. Neutralized cells were centrifuged to separate mature adipocytes and stromal-vascular fraction. Floating adipocytes were removed and pelleted stromal cells were filtered through a 100 μm cell strainer before plating. ADS cells were cultured in Dulbecco's modified Eagle's medium (DMEM) containing 10% fetal calf serum (FCS) at 37 °C in an atmosphere of 5% CO_2. Cells were grown to subconfluence and passaged by standard methods of trypsinization.

Pancreatic Islets were isolated from the rat pancreas[48]. Pancreas of SD rats was infused with 0.2% type V collagenase (Sigma), quickly excised, minced, and incubated at 37 °C for 30 min. Neutralized cells was washed in Hank's solution and centrifuged. Islets were separated using

Ficoll gradient centrifugation (Ficoll 400 DL, Sigma). Islets were cultured in DMEM containing 100 mL/L FCS, 200 kU/L penicillin, 100 mg/L streptomycin, and 2 mmol/L L-glutamine (Gibco) at 37 °C in an atmosphere of 5% CO_2. Medium was changed every second day.

3-D multicellular system construct and operation The ADS Cells were trypsinized off the culture dishes upon subconfluence, washed and quantified. Then cells were mixed with gelatin (Tianjin green-island Company), alginate (SIGMA) and fibrinogen (SIGMA) gel (gelatin: alginate: fibrinogen, 2:1:1) at a density of 3×10^7 cells/mL. After mixing, 1 mL of the mixture was loaded into a sterilized syringe (1mL, 0.45×16 RW LB). We used a software package (Microsoft, AT6400) to design the complex 3-D structure, which consisted of square grids and orderly channels about 400 um in diameter (Fig1 a). Following the designed structure, a refit nozzle controlled by computer was used to deposit the mixture on a glass chip at a temperature of 10 ℃ (Gelatin at gel state). The program was run 8 times consecutively at the same position to generation of a $10\times10\times2$ mm^3 3-D configuration with the square pattern. When the process was finished, the 3-D structure was crosslinked with 10% $CaCL_2$ for 1 min (crosslink the alginate), washed with DMEM three times. Then the 3-D structure was further stabilized by 50μU/ml Thrombin (crosslink the fibrinogen) in a culture medium containing DMEM, 10% FCS, 1 μmol/L insulin, EGF and 50 U/mL aprotinin (Sigma), placed in a CO_2 incubator at 37 ℃. After 3 days of culture, the medium was switched to another containing 10% FCS, 1 μM insulin, 1 μM dexamethasone, 0.5 mmol/L isobutyl-methylxanthine (IBMX; Sigma), and 50 u/mL aprotinin for 3 d. At the 6^{th} day, the pancreatic islets were aspirated and deposited at designated position of the 3-D structure. The medium was changed every other day. For 2-D control experiment, ADS cells were plated at 5×10^5 cells/well plates and induced to adipocytes by IBMX or to endothelial cells by EGF.

Structural analyses by Scanning electron microscopy At the 6^{th} day of culture, the multicellular 3-D structure were washed in phosphate buffer (pH 7.4) and fixed with 3% glutaraldehyde for 2 h. Then the samples were post-fixed with 0.5% OsO4 and rinsed with PB again. The samples were dried in vacuum freeze dryer for 12 h. After dehydrated, samples were sputter coated with gold–palladium. All micrographs were obtained in a scanning electron microscope (Hitachi S450, JAP)

Immunostaining For inmunofluorescence analyses, the assembled multicellular 3-D structure was fixed with 4% glutaraldehyde for 20 min at 20°C, and washed 3 times with PBS. The structure was incubated with 50 μg/mL propidium iodide (PI, sigma USA) for 20 min (nuclear staining), then the structure were incubate with primary antibodies: rabbit anti-rat:CD31 (1:20 in PBS); rabbit anti-rat CD34; rabbit anti-rat insulin (1:50) (all from Santa Cruz, USA) for 30 min respectively. And then the structure was incubated with a secondary antibody (FITC-conjugated anti rabbit IgG, Santa Cruz, 1:20 in PBS) for 30 min. Finally, the samples were washed with PBS and observed by fluorescence microscope (OLYMPUS BX51, JAP) or confocal microscopy (Leica TCS SP2, Germany). Image acquisition and analysis were performed using the Applied DP-Controller system (OLYMPUS, JAP) and Image-pro Plus 5.0 (Media Cybernetics, USA).

Dynamic insulin secretion experiment We measured Insulin secretion kinetics by perfusion experiments. After the islets were deposited in the structure, the structures were precultured in normal glucose (5 mM) or high glucose (15 mM) medium. After 5 days, islets in or not in the 3-D structures (20 islets/per) were introduced to a 1-mL perfusion chamber and exposed to flowing perfusate (DMEM, 0.2 mL/min) with a basal glucose concentration (2mM) for 1 h for islet cell starvation. Basal insulin secretion was estimated at the same medium and then switched to a high glucose content (15 mM) perfusate and collected every 2 min for 20 min. Then the perfusate was returned to the basal solution and collected every 5 min for 15 min. The insulin content of collected samples was measured by using a rat insulin ELISA kit according to the manufacturers instructions (RB, USA) by a microplate reader (Bio-Rad 550). For drug experiment, rosiglitazone (3 μg/mL) and nateglinide (5 μg/mL) were added to the culture medium at the 11^{th} day respectively.

Measurement of Glucose consumption, FFA release, and Adipogenesis After seeding the islets, the multicellular 3-D system was further cultured in normal glucose (5 mM) or high glucose (15 mM) medium for more than 7 d. At the 13^{th} day, we replaced the medium with DMEM containing 25 mM glucose. After 24 h, we collected the medium for the measurement of glucose consumption. Glucose concentration was measured by Glucose assay kit, (Biovision,

USA). Glucose consumption rates were calculated subtracting residual glucose in the treated medium from glucose in nontreated medium. For determination of FFA release, we replace the medium with DMEM containing 2% fatty acid free BSA and 10 μM isoproterenol at the 15th day. Aliquots of the medium were collected and the FFA content was measured with FFA assay kits (Nanjing Jiancheng, PRC). For drug experiment, rosiglitazone was added to the culture medium at the 11th day.

We use oil red o staining to indicate the high glucose-induced adipogenesis of adipocyte. After seeding the islets, the 3-D multicellular system was cultured in normal glucose (5 mM) or high glucose (15 mM) medium for more than 8 d. At the 14th d, the 3-D multicellular system was fixed with 10% formalin, stained with 0.1 mg/mL oil red O solution for 2 h. Oil red O dye was extracted into isopropanol and absorbance was measured at 510 nm. For drug experiment, rosiglitazone (3 μg/mL) was added to the culture medium at the 7th day.

Measurement of Adipocytokine by ELISA After seeding the islets, the multicellular 3-D system was cultured in normal glucose (5 mM) or high glucose (15 mM) medium, three day-conditioned media were harvested at the 21th day. Leptin, resistin and adiponectin were measured in cell culture media using rat leptin ELISA kits (RB, USA), rat resistin ELISA kits (TPI, USA) and rat adiponectin ELISA kits (USCNLIFE, USA) respectively. The assays were conducted in 96-well microplates according to the manufacture's recommendations, with a microplate reader. Results were expressed as a rate of adipocytokine level to DNA content of the cells. Adipocytes in 2-D culture and in 3-D culture without islets were deal with the same process. For drug experiment, rosiglitazone (3 μg/mL) was added to the culture medium at the 12th day.

DNA assays Following the measurement of adipocytokine, samples and cell-free structure were carefully collected and homogenized, and then digested (0.14 mg/mL papainase in 100 mM phosphate buffer with 10mM ethylenediaminetetraacetate, EDTA, and 10 mM cysteine) for 20 h at 60 °C, using 2 mL of the enzyme solution per sample [42]. DNA content was determined fluorimetrically following the binding of Hoechst 33258 dye (Sigma) using calf thymus type I DNA as a standard [61]. The fluorescence of negative, cell-free structure was subtracted from the fluorescence values of experimental groups to account for fluorescence of the material alone.

Measurement of ET-1 and NO. After seeding the islets, the multicellular 3-D system was culture with 5 mM glucose. At the 13th day, the medium were replaced with DMEM containing 25 mM glucose. Two day-conditioned media were harvested at the 15th day. ET-l released into the culture media was measured by ELISA kit (RB, USA) according to the manufacturer's instructions. NO concentrations in the culture media were detected by using NO Detection kit (JinMei Biotech Co. Ltd.) based on nitrate reductase method. Endothelial cells in 2-D culture and in 3-D culture without islets were dealt with the same process. For drug experiment, rosiglitazone (3 μg/ml) was added to the culture medium at the 10th day.

Statistical analysis. Statistical analysis was performed by Student's *t*-test using both confidence interval estimate analysis and t score probability hypothesis testing method for two independent sample groups. However, there is a considerable probability of statistical error due to the limited numbers of subjects in this study.

ACKNOWLEDGEMENTS

This study was supported by the National Natural Science Foundation of China (Grant No. 30600140,30440043 and 30400099), the National Natural Science Foundation of China / the Research Grants Council of Hong Kong (Grant No.50731160625), the National Post-doctor Foundation of China (Grant No. 20060390074). The authors gratefully thank Beijing Municipal Science & Technology Commission for its contribution to this project (Grant No. H060920050530).

COMPETING INTERESTS STATEMENT

The authors declare that they have no competing financial interests.

References

1. Smith, C.M., Christian, J.J., Warren, W.L. & Williams, S.K. Characterizing environmental factors that impact the viability of tissue-engineered constructs fabricated by a direct-write bioassembly tool. *Tissue Eng*. **13**, 373-83. (2007).

2. Paul, C. MATERIALS SCIENCE: Printing Cells, *Science* **318**, 208 – 209 (2007).
3. Boland, T., Mironov, V., Gutowska, A., Roth, E.A. & Markwald, R.R. Cell and organ printing 2: fusion of cell aggregates in three-dimensional gels. *Anat Rec B New Anat.* **272**, 497-502 (2003).
4. Wang, X.H., Yan, Y.N., & Zhang, R.J. Rapid prototyping as tool for manufacturing bioartificial livers. *Trends Biotechnol.* **25**, 505-513 (2007).
5. Yan, Y.N. *et al*. Fabrication of viable tissue-engineered constructs with 3-D cell-assembly technique. *Biomaterials*. **26,** 5864–5871 (2005).
6. Wang, X.H. *et al*. Generation of three-dimensional hepatocyte/gelatin structures with rapid prototyping system *Tissue Eng.* **12**, 83-90 (2006).
7. Lysaght, M. J. & Hazlehurst, A. L. Tissue engineering: the end of the beginning. *Tissue Eng*. **10**, 309–320 (2004).
8. Griffith, L.G. & Naughton, G.. Tissue engineering—current challenges and expanding opportunities. *Science* **295**, 1009–1014 (2002).
9. Griffith LG, & Swartz MA. Capturing complex 3D tissue physiology in vitro. *Nat Rev Mol Cell Biol.* **7**, 211-224 (2006).
10. Suuronen, E. J., Sheardown, H., Newman, K. D., McLaughlin, C. R. & Griffith, M. Building in vitro models of organs. *Int. Rev. Cytol*. **244**, 137–173 (2005).
11. Sivaraman, A. *et al*. A microscale in vitro physiological model of the liver: predictive screens for drug metabolism and enzyme induction. *Curr. Drug Metab.* **6**, 569–592 (2005).
12. Bleicher, K.H. et al. Hit and lead generation: beyond high-throughput screening. *Nat Rev Drug Discov.* **2**, 369-378 (2003).
13. Haney, S.A., LaPan, P., Pan, J, & Zhang J. High-content screening moves to the front of the line. *Drug Discov Today.* **11**, 889-894 (2006).
14. Basu, S. *et al*. A synthetic multicellular system for programmed pattern formation. *Nature.* **434,** 1130-1134 (2005).
15. Hotary, K.B. *et al*. Membrane type I matrix metalloproteinase usurps tumor growth control imposed by the three-dimensional extracellular matrix. *Cell.* **114**, 33-45 (2003).
16. Weaver, V.M. *et al*. b4 integrin–dependent formation of polarized threedimensional architecture confers resistance to apoptosis in normal and malignant mammary epithelium. *Cancer Cell.* **2**, 205–216 (2002).
17. Metabolic syndrome. *Nat Med*. **12**, 26 (2006).
18. Despres, J.P. & Lemieux, I. Abdominal obesity and metabolic syndrome. *Nature.* **444**, 881-887 (2006).
19. Grund, S.M. Drug therapy of the metabolic syndrome: minimizing the emerging crisis in polypharmacy *Nat Rev Drug Discov.* **5**, 295-309 (2006).
20. Kuo, L.E., *et al*. Neuropeptide Y acts directly in the periphery on fat tissue and mediates stress-induced obesity and metabolic syndrome. *Nat Med*. **13**, 803-811 (2007)

21. Shoelson, S.E. Banking on ATM as a new target in metabolic syndrome. *Cell Metab.* **4,** 337-338 (2006).
22. Guarente, L. Sirtuins as potential targets for metabolic syndrome. *Nature*. **444**, 868-874 (2006)
23. Xu, M.E. *et al*..A preadipocyte differentiation assay as a method for screening potential anti-type II diabetes drugs from herbal extracts. *Planta Med.* **72**, 14-19 (2006).
24. Alemzadeh, R., & Tushaus, K.M. Modulation of adipoinsular axis in prediabetic zucker diabetic fatty rats by diazoxide. *Endocrinology*. **145**, 5476-5484 (2004).
25. Caballero, A.E.. Endothelial dysfunction in obesity and insulin resistance: a road to diabetes and heart disease. *Obes Re.s* **11**, 1278–1289. (2003)
26. Cowan, C.M., *et al*. Adipose-derived adult stromal cells heal critical-size mouse calvarial defects. *Nat Biotechnol.* **22**, 560-567 (2004).
27. Zuk, P.A. *et al*. Human adipose tissue is a source of multipotent stem cells. *Mol. Biol. Cell* **13**, 4279–4295 (2002).
28. Pratley, R.E. & Weyer, C. The role of impaired early insulin secretion in the pathogenesis of type II diabetes mellitus. *Diabetologia.* **44**, 929– 945 (2001).
29. Sonya, M., *et al*. Impaired β-cells Functions Induced by Chronic Exposure of Cultured Human Pancreatic Islets to High Glucose *Diabetes*. **48**, 1230-1236 (1999).
30. Buckingham, R.E. *et al*. Peroxisome proliferator-activated receptor-gamma agonist, rosiglitazone, protects against nephropathy and pancreatic islet abnormalities in Zucker fatty rats. *Diabetes.* **47**, 1326-1334 (1998).
31. Hollander, P.A. *et al*. Importance of early insulin secretion: comparison of nateglinide and glyburide in previously diettreated patients with type 2 diabetes, *Diab. Care*. **24**, 983–988 (2001).
32. Boden, G., *et al*. Combined use of rosiglitazone and fenofibrate in patients with type 2 diabetes: prevention of fluid retention. *Diabetes*. **56**, 248-255 (2007).
33. Oakes, N.D. *et al*. A new antidiabetic agent, BRL 49653, reduces lipid availability and improves insulin action and glucoregulation in the rat. *Diabetes*. **43**, 1203-1210 (1994).
34. MacDougald, O.A. & Burant, C.F. The rapidly expanding family of adipokines. *Cell Metab*. **6**, 159-161. (2007).
35. Leiter, E.H, *et al*. Differential endocrine responses to rosiglitazone therapy in new mouse models of type 2 diabetes. *Endocrinology.* **147**, 919-26 (2006).
36. Samaha, F.F. *el al*. Effects of rosiglitazone on lipids, adipokines, and inflammatory markers in nondiabetic patients with low high-density lipoprotein cholesterol and metabolic syndrome. *Arterioscler Thromb Vasc Biol*. **26**, 624-630 (2006).
37. Wang, T.D. *et al*. Relation of improvement in endothelium-dependent flow-mediated vasodilation after rosiglitazone to changes in asymmetric dimethylarginine, endothelin-1, and C-reactive protein in nondiabetic patients with the metabolic syndrome.. *Am J Cardiol.* **98**,

1057-1062 (2006).

38. Potenza, M.A., Marasciulo, F.L., Tarquinio, M., Quon, M.J. & Montagnani, M. Treatment of spontaneously hypertensive rats with rosiglitazone and/or enalapril restores balance between vasodilator and vasoconstrictor actions of insulin with simultaneous improvement in hypertension and insulin resistance. *Diabetes.* **55**, 3594-603 (2006).
39. Mueller-Klieser, W. Three-dimensional cell cultures: from molecular mechanisms to clinical applications. *Am. J. Physiol.* **273**, C1109–C1123 (1997).
40. Benya, P.D. & Shaffer, J.D. Dedifferentiated chondrocytes reexpress the differentiated collagen phenotype when cultured in agarose gels. *Cell.* **30,** 215–224 (1982).
41. Kang, X., Xie, Y. & Kniss, D.A. Adipose Tissue Model Using Three-Dimensional Cultivation of Preadipocytes Seeded onto Fibrous Polymer Scaffolds. *Tissue Eng.* **11**, 458-468 (2005).
42. Zuk, P.A. *et al*. Multilineage cells from human adipose tissue: implications for cell-based therapies. *Tissue Eng*. **7**, 211–228 (2001).
43. Jain, R.K., Au, P., Tam, J., Duda, D.G. & Fukumura, D. Engineering vascularized tissue. *Nat Biotechnol.* **23**, 821-823. (2005).
44. Hwang, C.S., Loftus, T.M., Mandrup, S. & Lane, M.D. Adipocyte differentiation and leptin expression. *Rev Cell Dev Biol.* **13**, 231-259 (1997).
45. Wang, X.L., *et al*. Free fatty acids inhibit insulin signaling-stimulated endothelial nitric oxide synthase activation through upregulating PTEN or inhibiting Akt kinase. *Diabetes.* **55**, 2301-2310 (2006).
46. Boden, G. & Shulman, G.I. Free fatty acids in obesity and type 2 diabetes: defining their role in the development of insulin resistance and beta-cell dysfunction. *Eur J Clin Invest*. Suppl **3**, 14-23 (2002)
47. Halvorsen, Y.D. *et al*. Thiazolidinediones and glucocorticoids synergistically induce differentiation of human adipose tissue stromal cells: biochemical, cellular, and molecular analysis. *Metabolism*. **50**, 407–413 (2001).
48. Lacy, P.E. & Kostianovsky, M. Method for the isolation of intact islets of Langerhans from the rat pancreas. *Diabetes*. **16**, 35-39 (1967).

Figure 1 | Construct and analyses of the multicellular 3-D system. **(a)** ADS cells in prepolymer solution were loaded into a sterilized syringe (1) Computer controlled a refit nozzle to deposit the mixture on a glass chip at a temperature of 10 ℃ and generated a 3-D structure, which consisted of square grids and orderly channels. (2) The 3-D structure was crosslinked by $CaCL_2$ and thrombin respectively, cells embedded in the matrices had a relatively stable micro environment. The structure was removed and cultured. (3) At the 7^{th} days, the pancreatic islets were deposited into designated micro holes in the structure. **(b)** The 3-D structure

cultured in a plate. **(c)** Immunostaining of the 3-D structure using mAbs for CD34+ cells in green. **(d)** Scanning electron micrographs showed the development of extensive ECM and cell networks in the structure after 6 days of culture. **(e)** Immunostaining of the pancreatic islets in the 3-D structure using anti-insulin in green. 90% of the pancreatic islets can keep integrity globoid shapes for more than three weeks in the structure, **(f)** some envelopes of islets were broken, but the β-cells still congregated and kept secreting insulin.

Figure 2 | ADS cells in the 3-D structure could be controlled differentiation into endothelial cells and adipocytes. **(a, b)** Immunostaining of the 3-D structure using mAbs for CD34+ cells (ADS cells and endothelial cells) in green and PI for nuclear in red. **(c-f)** Immunostaining of the 3-D structure using mAbs for CD31+cells (mature endothelial cells) in green and PI for nuclear in red. ADS cells in the 3-D structure were cultured with EGF **(a, c, e, f)** or without EGF **(b, d)**. Image of **(e, f)** was observed by confocal microscopy. **(g, h)** Immunostaining of the 3-D structure using mAbs for CD31+ cells in green and Oil red O staining of the 3-D structure for adipocytes in red. ADS cells in 3-D structure were culture with EGF **(g)** or without EGF **(h)** for three days, and then treated with insulin, IBMX and dexamethasone.

Figure 3 | Insulin secretion kinetics of **(a)** the free islet, **(b)** the islet assembled in the 3-D structure were measured by perfusion experiments. Cells were incubated in normal glucose (**NG,** 5 mM) or high glucose (**HG**, 15 mM) for 5 d. For drug experiment, rosiglitazone (**ROS**, 3 μg/ml) or nateglinide (**NATE,** 5 μg/ml) were added to the **HG** culture medium at the 4^{th} day. Next the cells were introduced to a perfusion chamber and exposed to flowing perfusate with a basal glucose concentration (2mM) for 1h and then switched to a high glucose content (15 mM) perfusate for 20 min. Then the perfusate was returned to basal glucose concentration. The insulin content in the extracts was determined by ELISA insulin kit. Data are mean±s.d., n=3.

Figure 4 | Measurement of Glucose metabolism and lipid metabolism. Long-term exposure to high glucose **(HG** 15 mM**)** was used to induce the pathological changes of the cells in different culture system. For drug experiment, rosiglitazone (**ROS**, 3 μg/ml) was added to the HG culture medium. **(a)** Glucose consumption of cells was stimulated with 25 mM glucose and the glucose

concentration of the medium was measured with Glucose assay kit. **(b)** FFA release of cells was stimulated with isoproterenol (10 μM) and the FFA content was measured with FFA assay kits. Results were expressed as the ratios of the stimulate level to base level. (**c**) Adipogenesis.was stimulated by long exposure to HG and the lipid accumulation was measured with oil red o assay. Absorbance is designated as 1.0 for cell cultured in normal glucose. Data are mean±s.d., n=6.

Figure 5 | Adipocytokine secretion of adipocytes in different culture systems. Long-term exposure to high glucose **(HG** 15 mM**)** was used to induce the pathological changes of the cells in different culture system. For drug experiment, rosiglitazone (**ROS**, 3 μg/ml) was added to the HG culture medium. Adipocytokine secretion of adipocytes in different culture system: (**a**) leptin secretion (**b**) resistin secretion (**c**) adiponectin secretion. Adipocytokine content in the medium was determined by ELISA kit. Results were expressed as the ratios of the adipocytokine secretion level to the DNA content of the cells. Data are mean±s.d., n=6.

Figure 6 | Endothelin-1 and NO secretion of endothelial in different culture systems. Cells were cultured with high glucose (**HG** 25 mM) for two days. **(a)** Endothelin-1 concentrations in the culture medium were measured by ELISA kit. **(b)** NO concentrations in the culture medium were detected by NO Detection kit. For drug experiment, rosiglitazone (3 μg/ml) was added to the HG culture medium. Results were expressed as fold increase to base level. Data are mean±s.d., n=6.

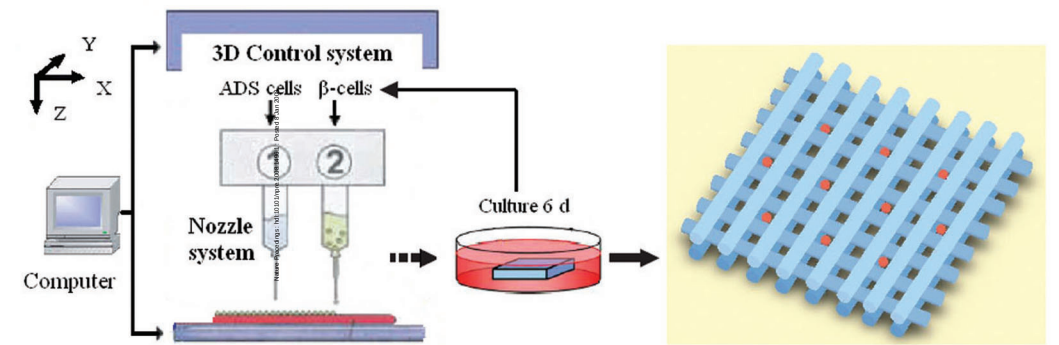
Y
X
Z
3D Control system
ADS cells
β-cells
1
2
Nozzle system
Computer
Culture 6 d

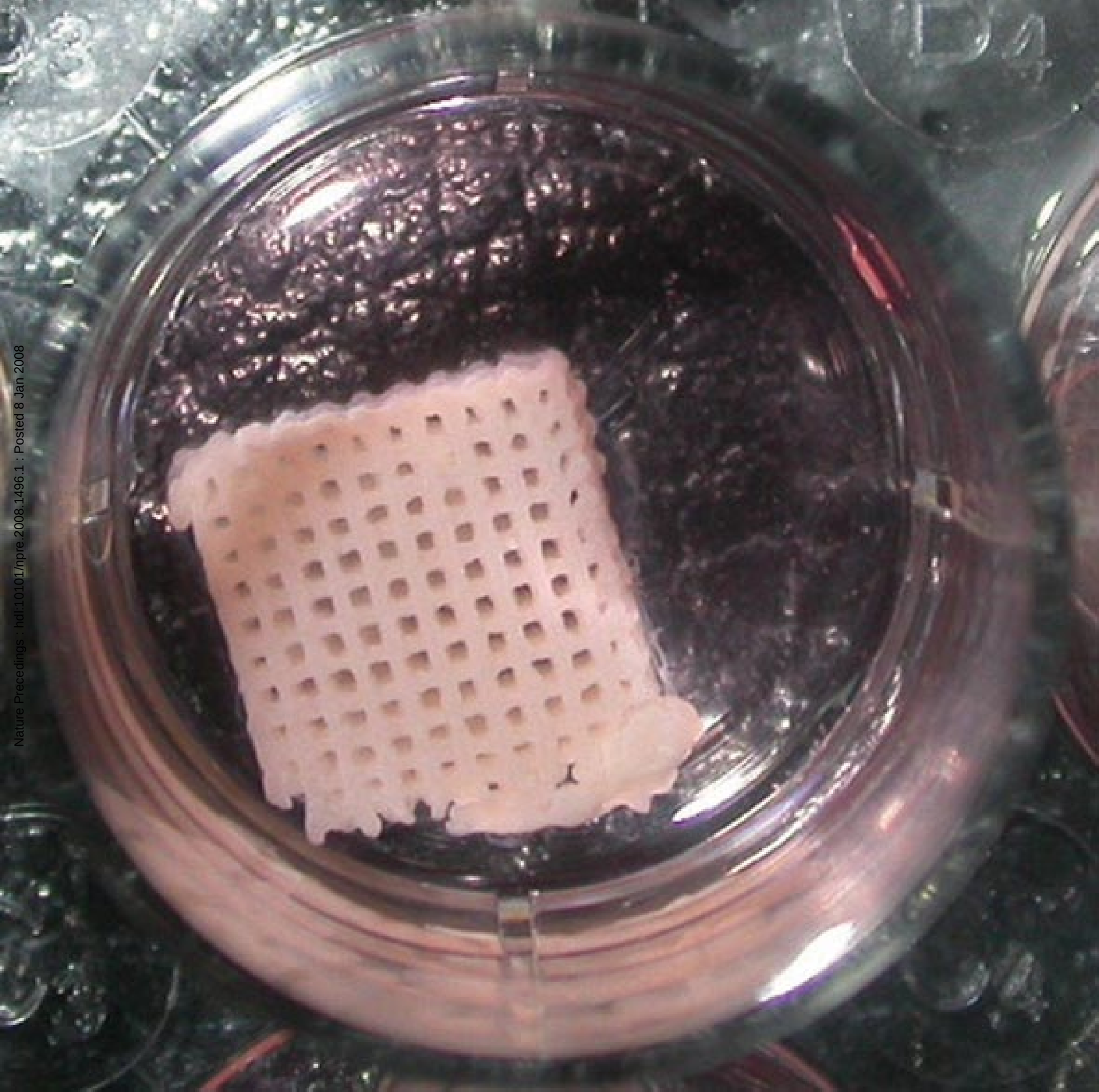

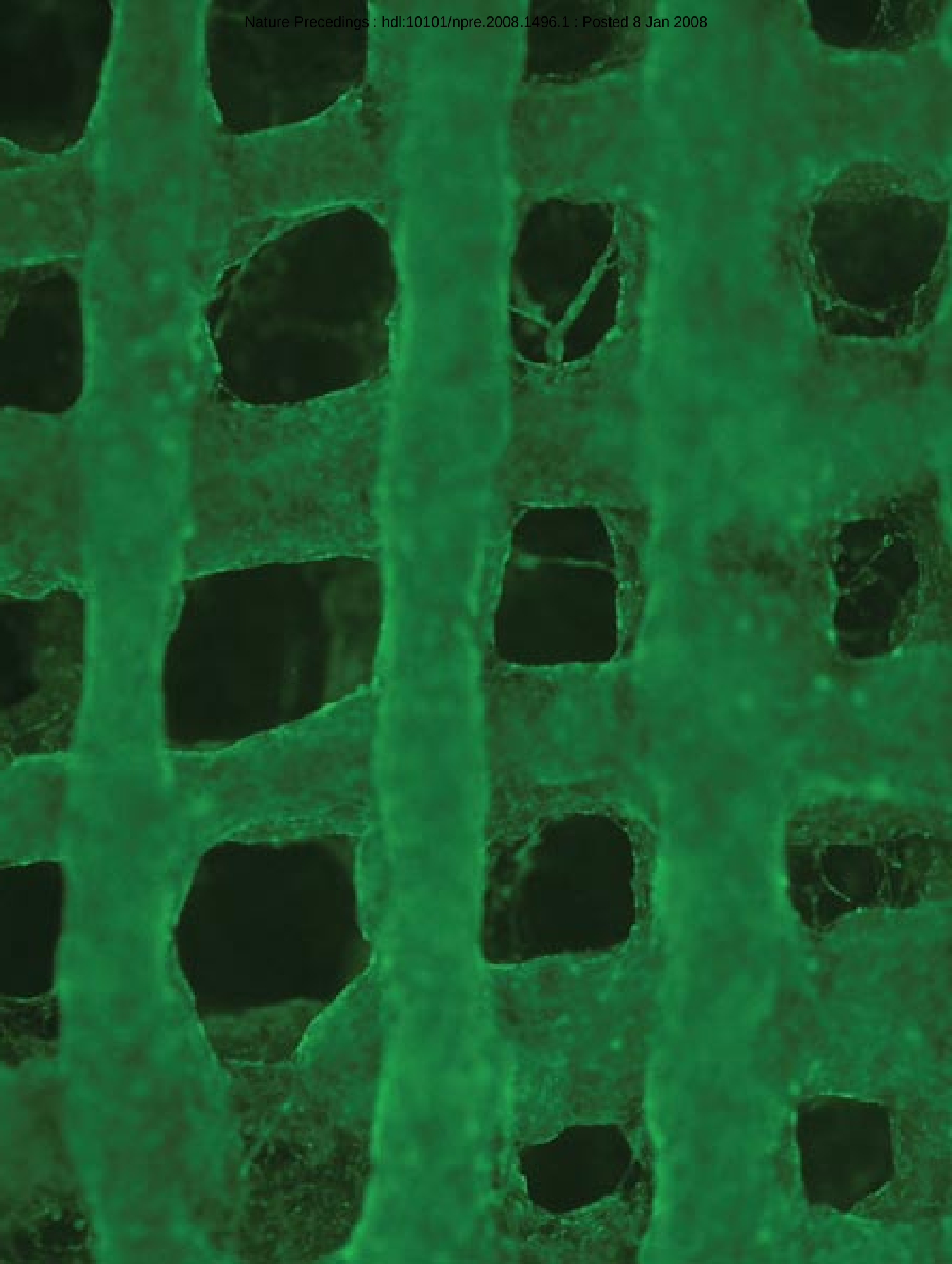

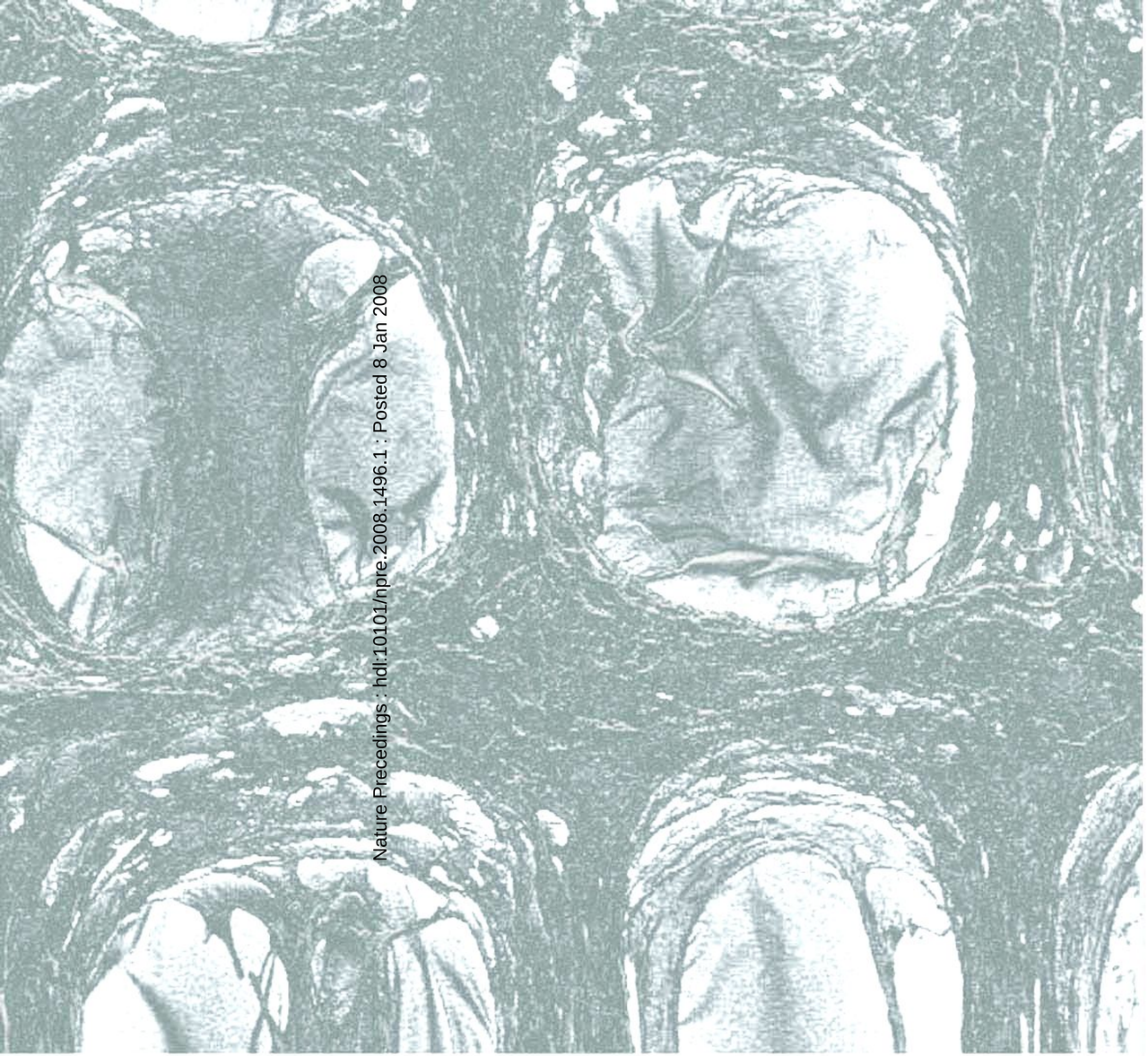

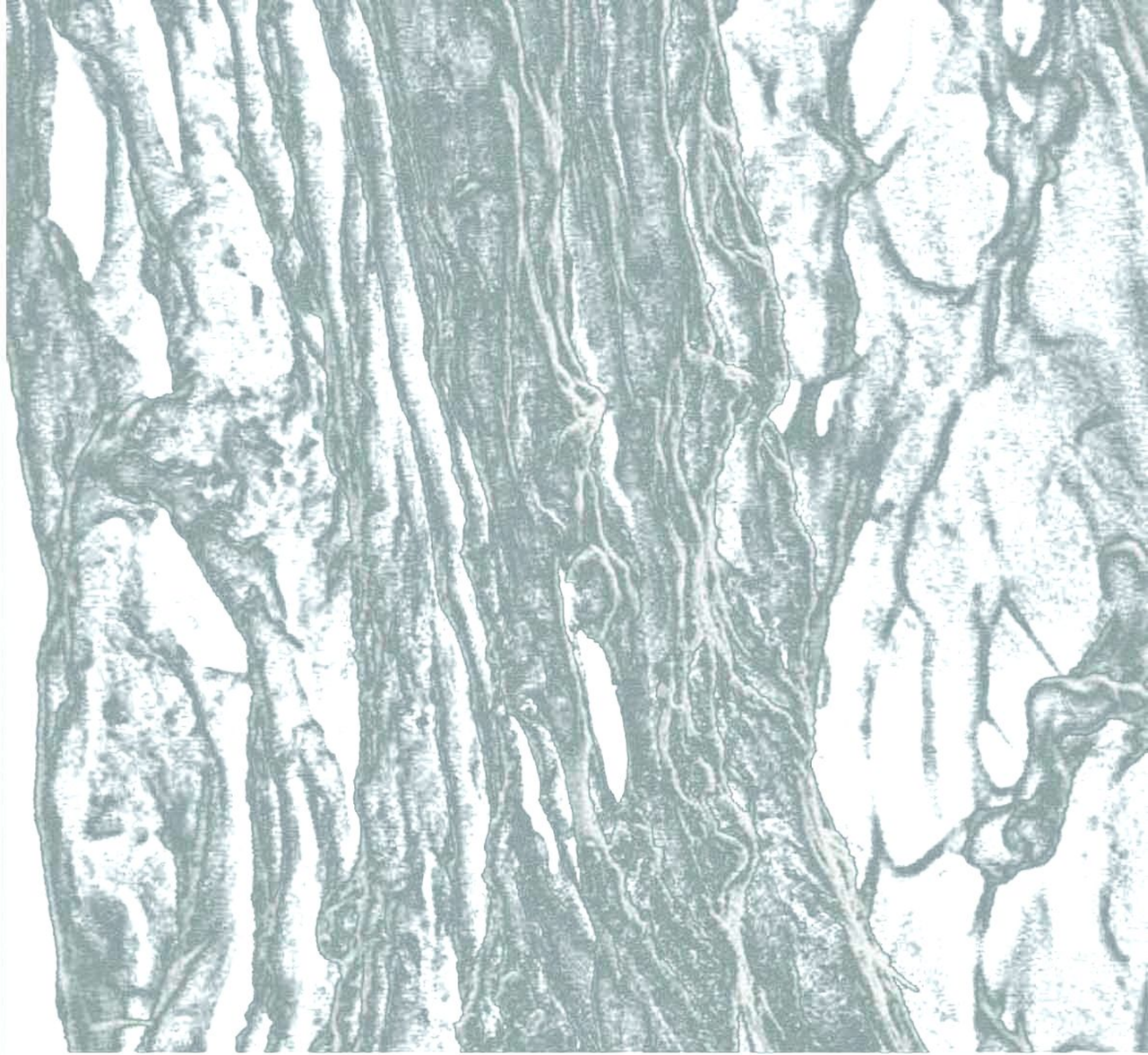

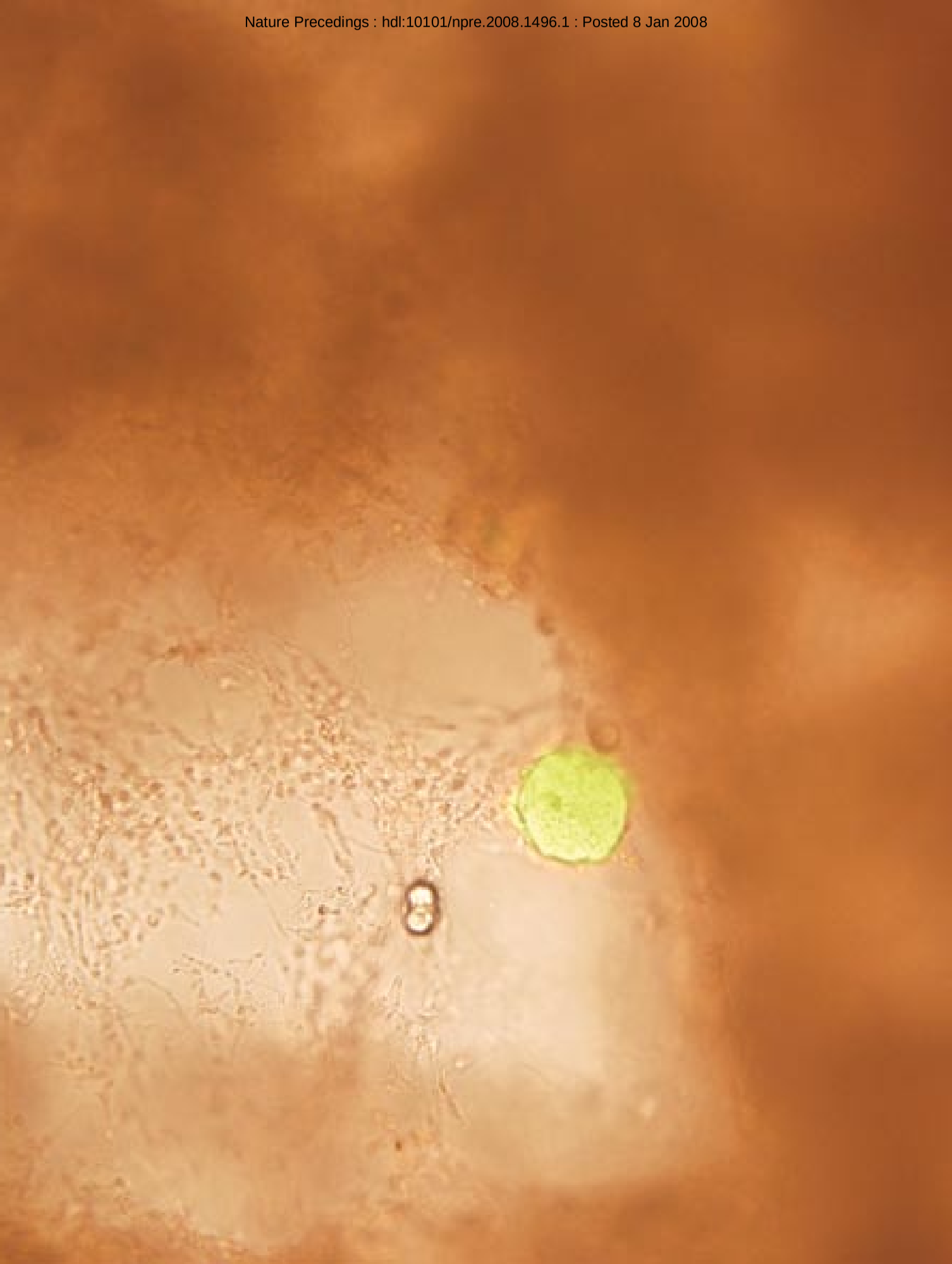

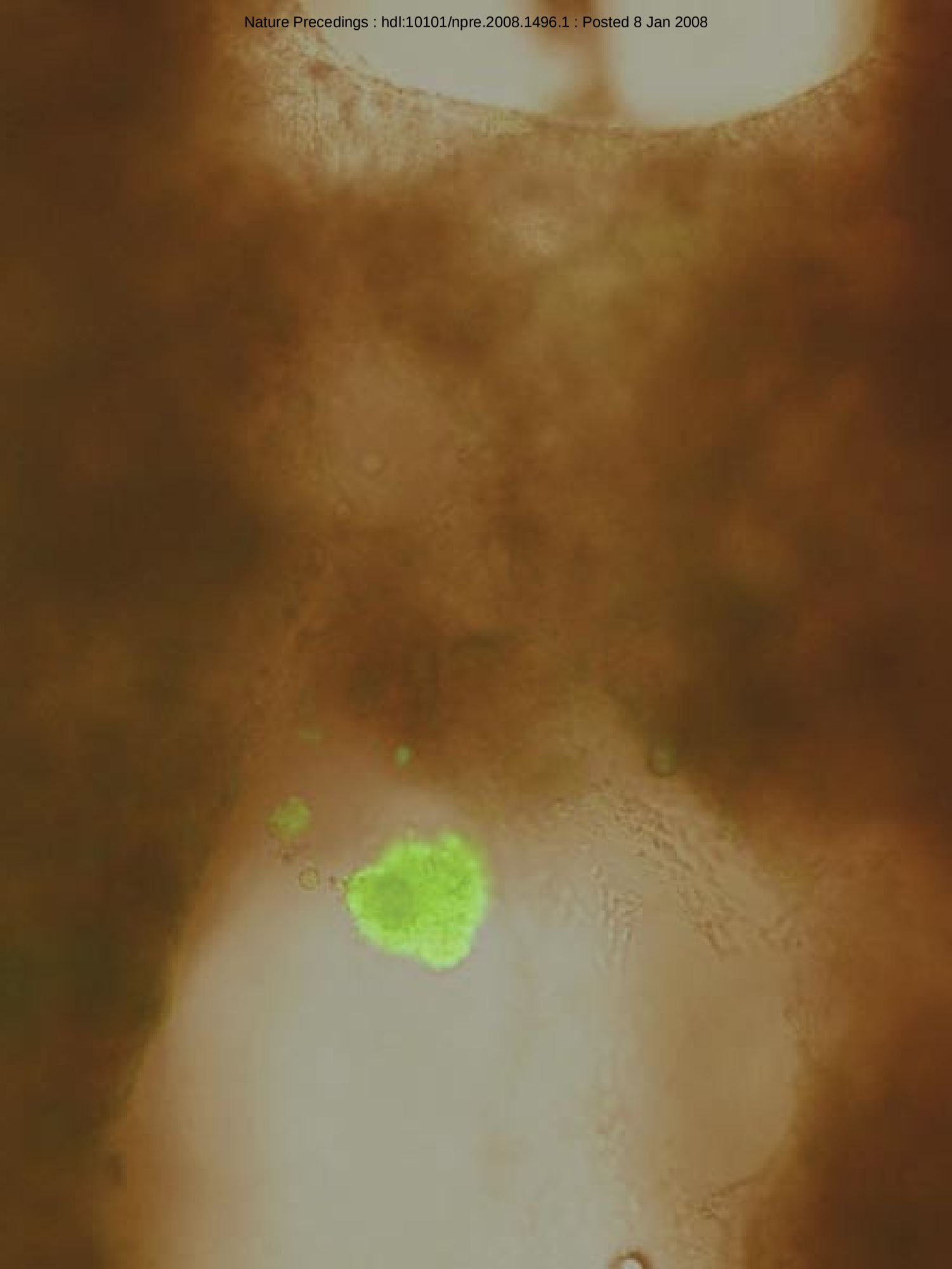

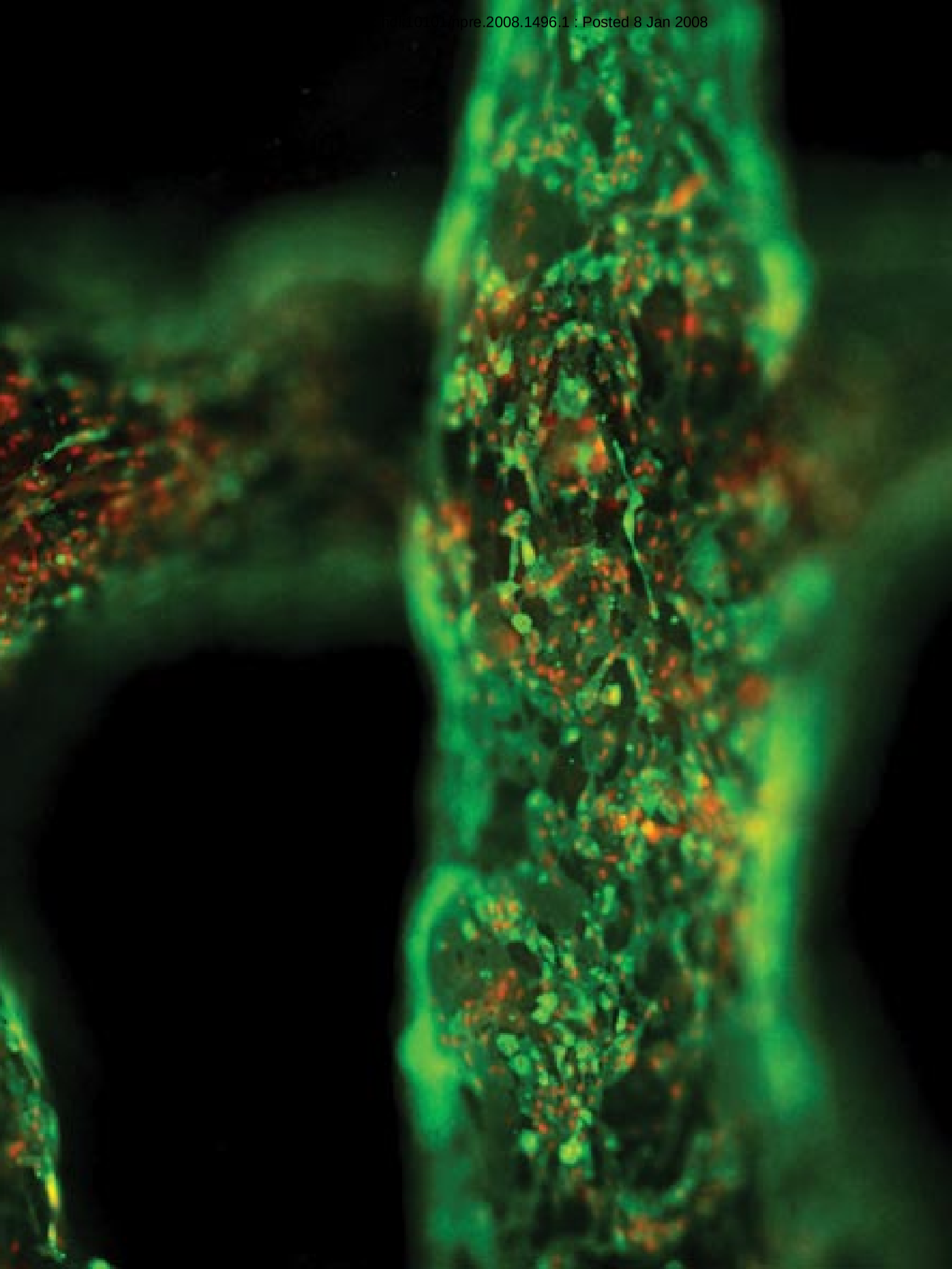

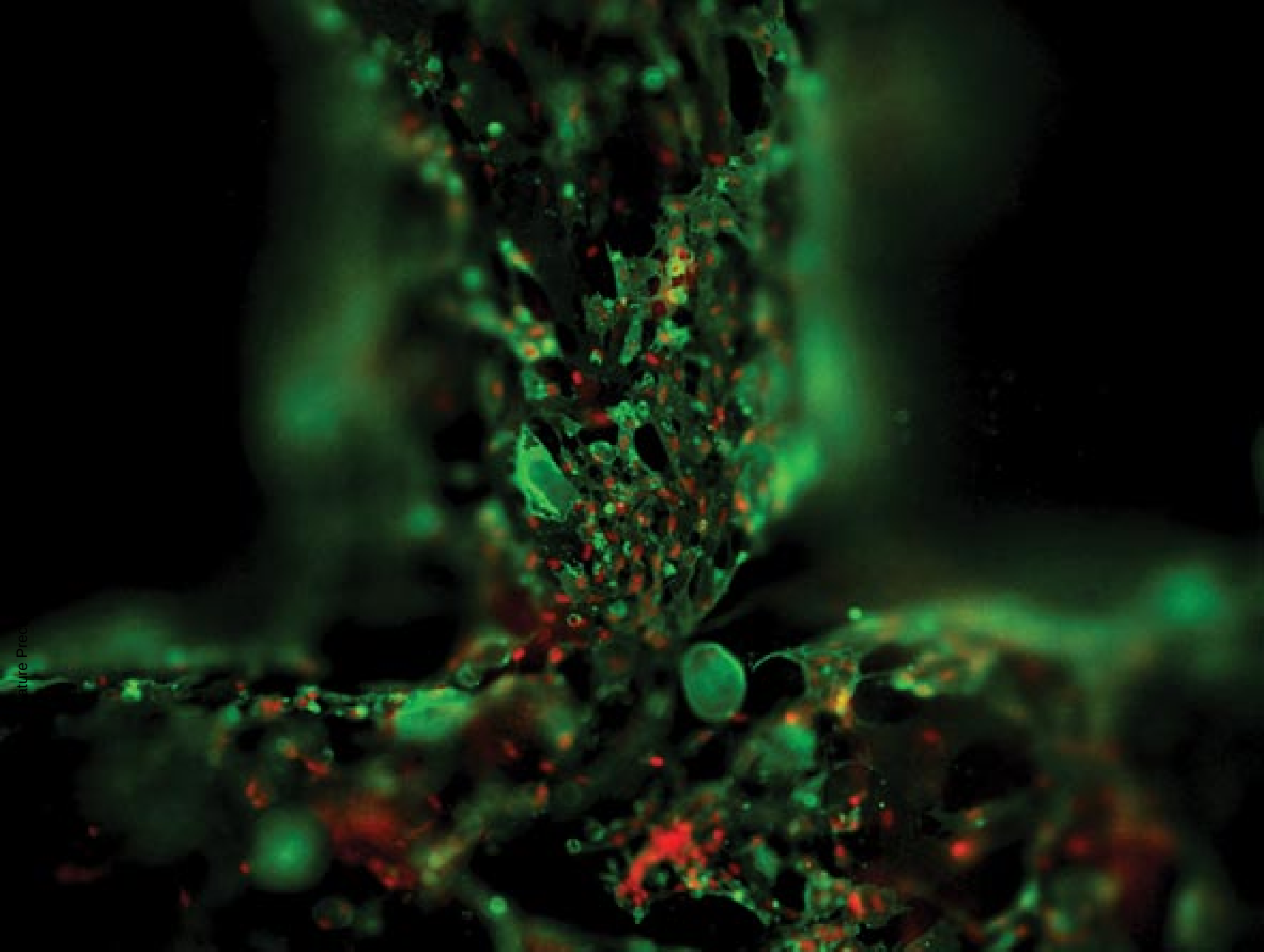

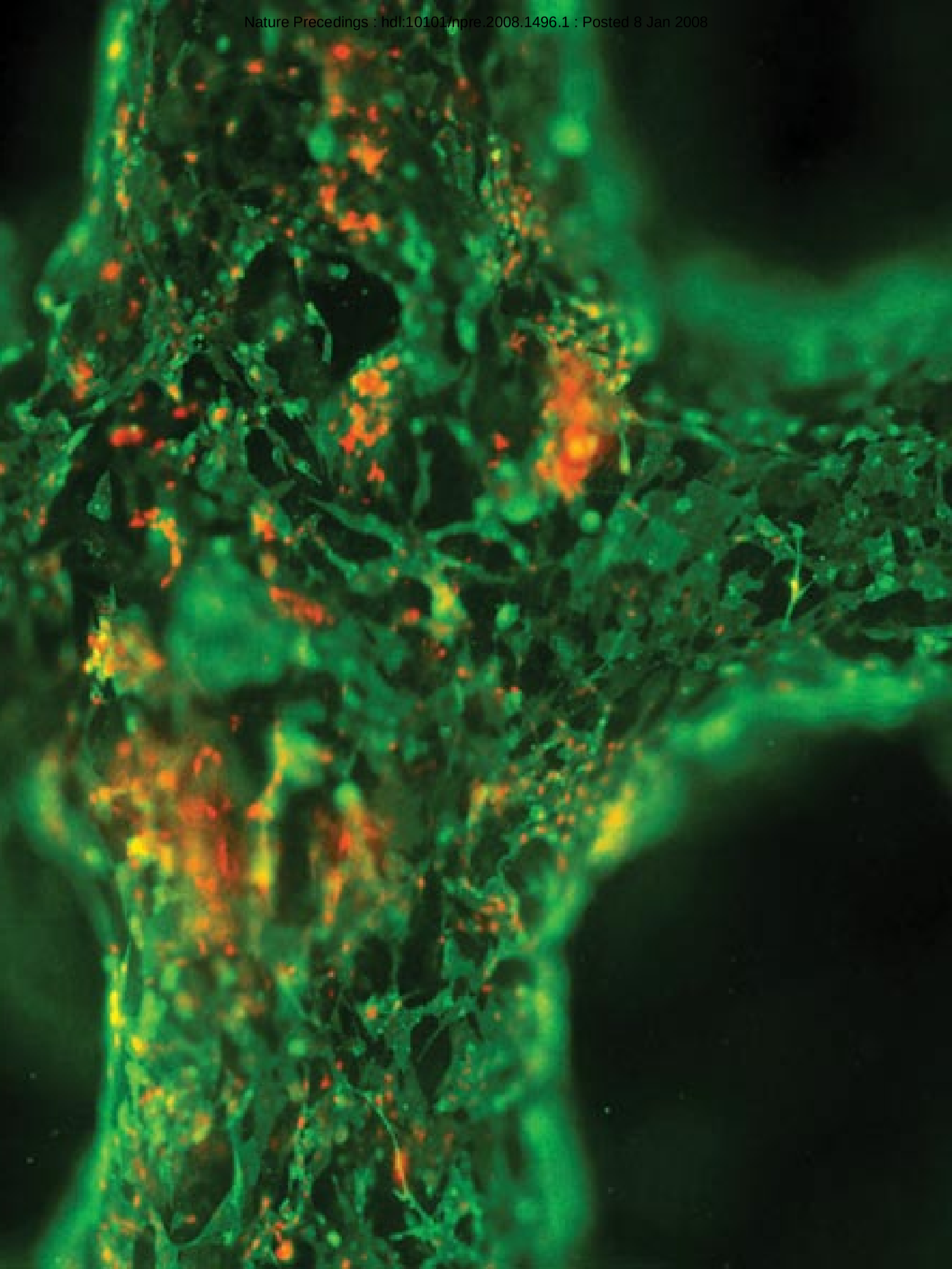

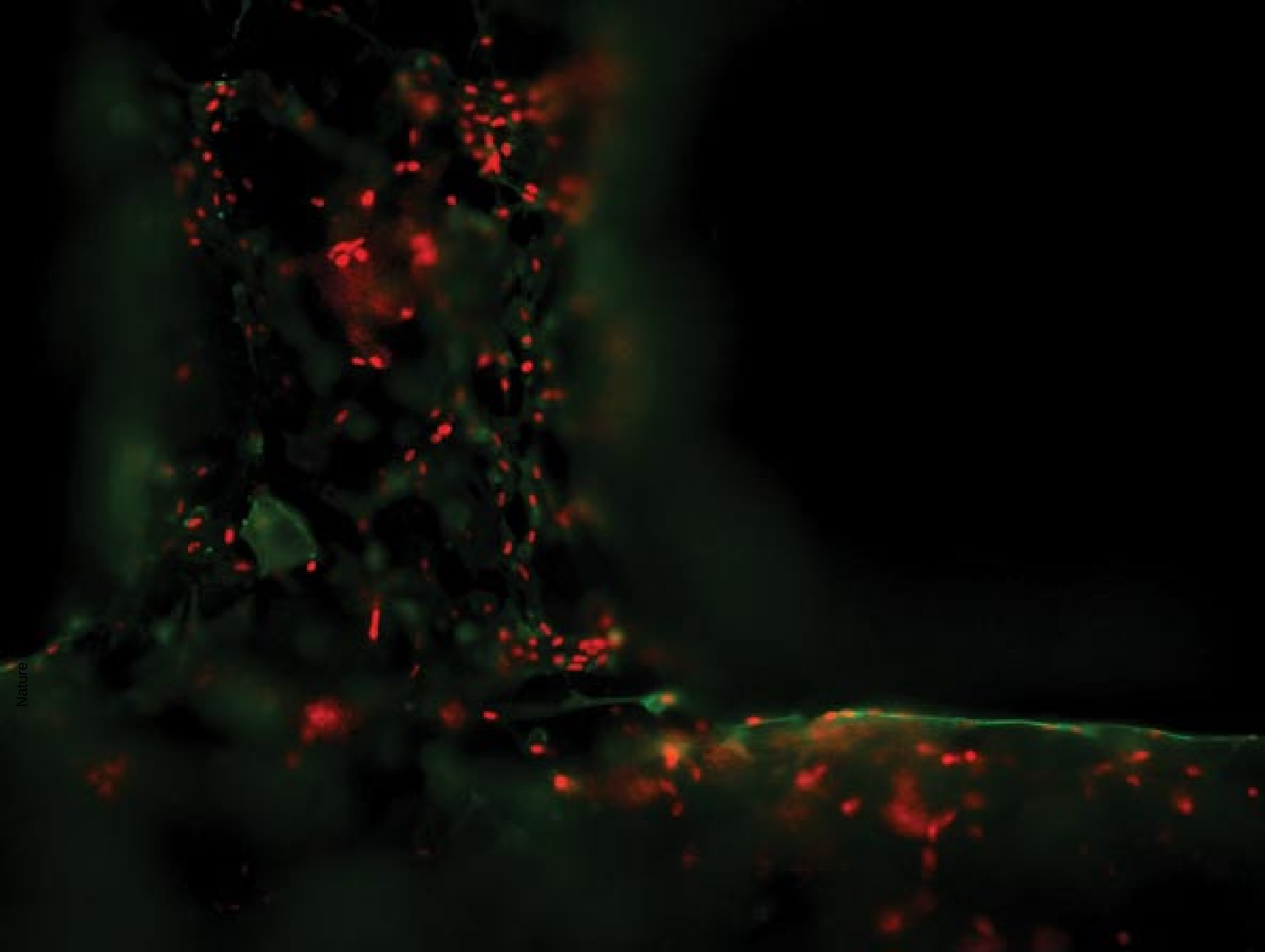

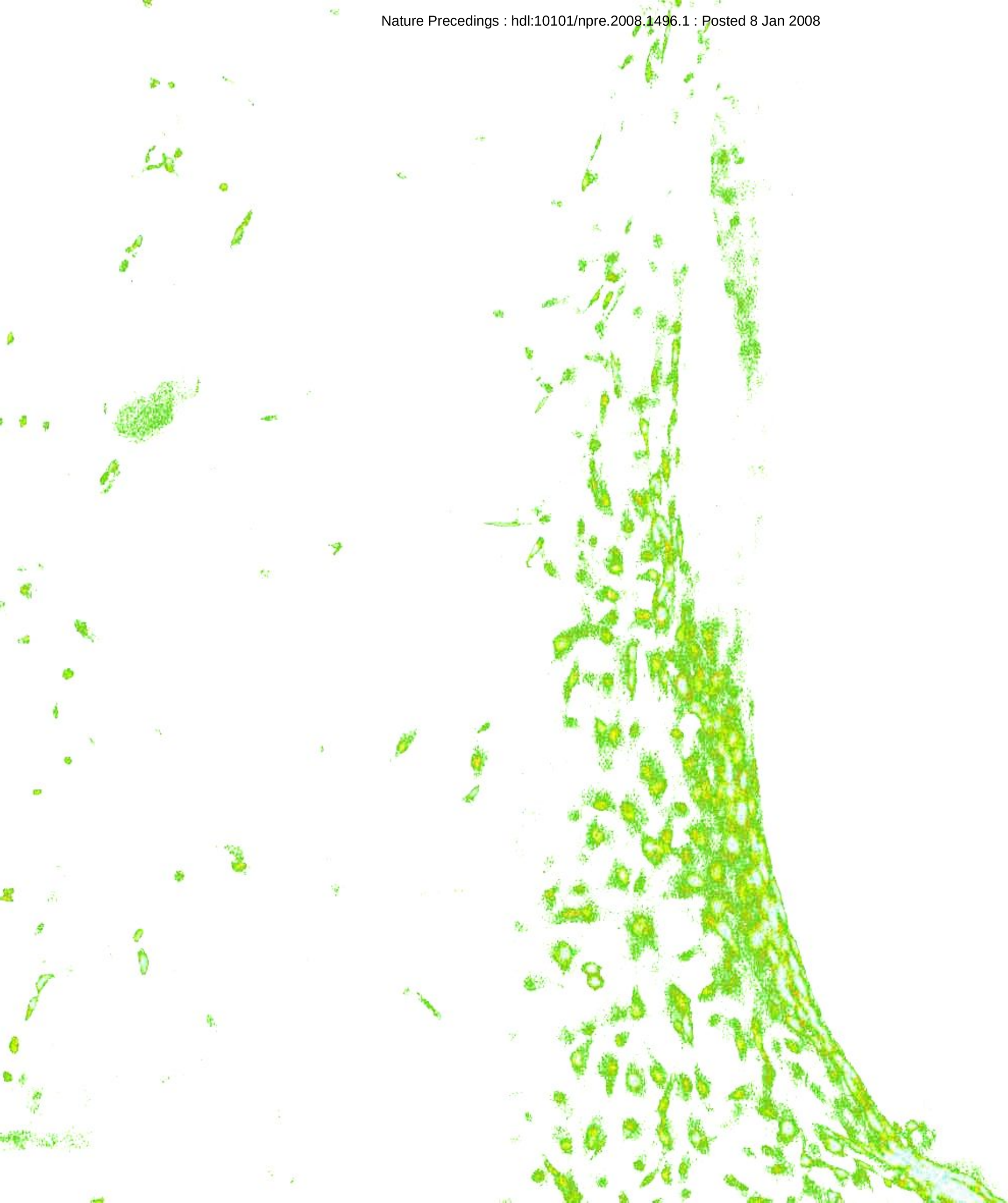

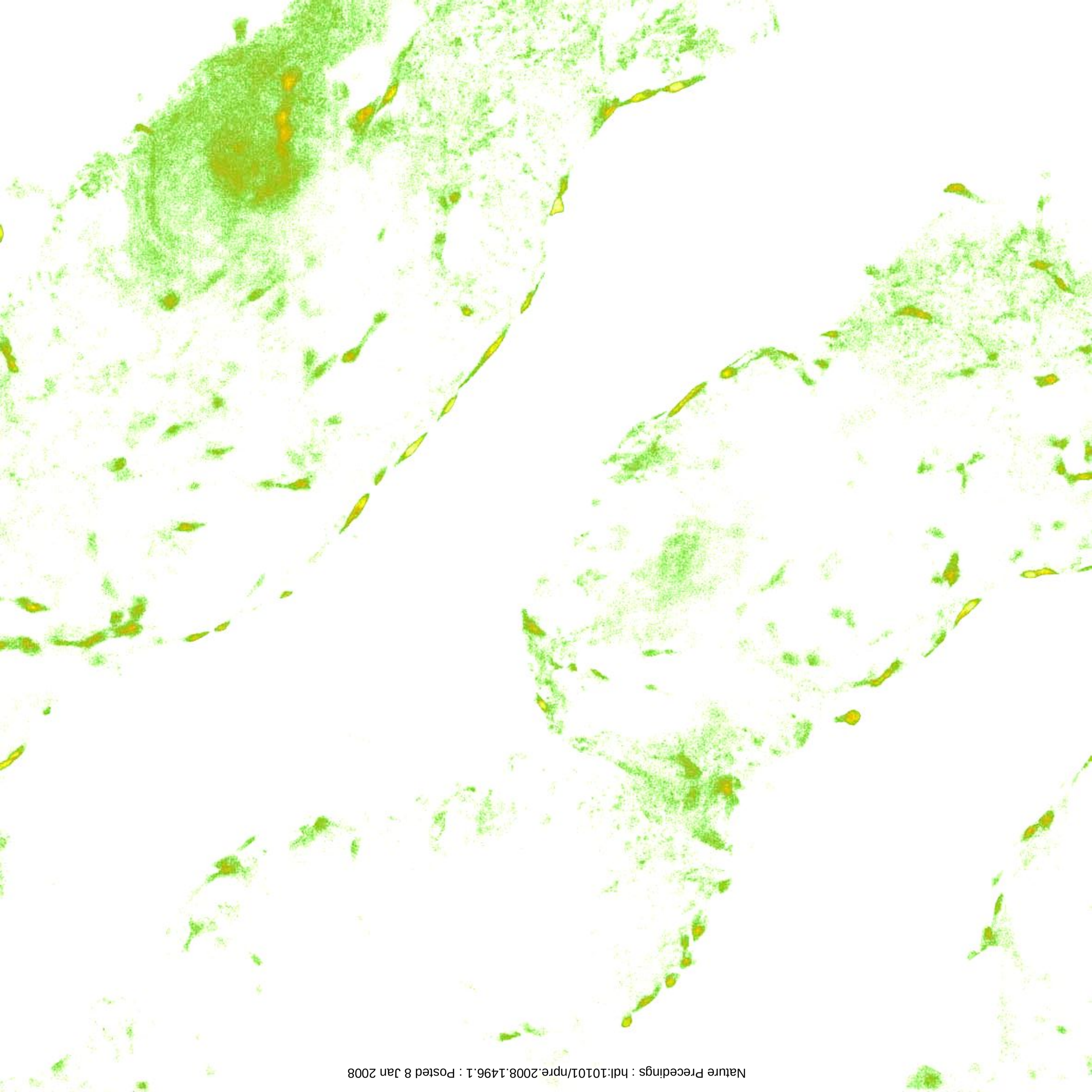

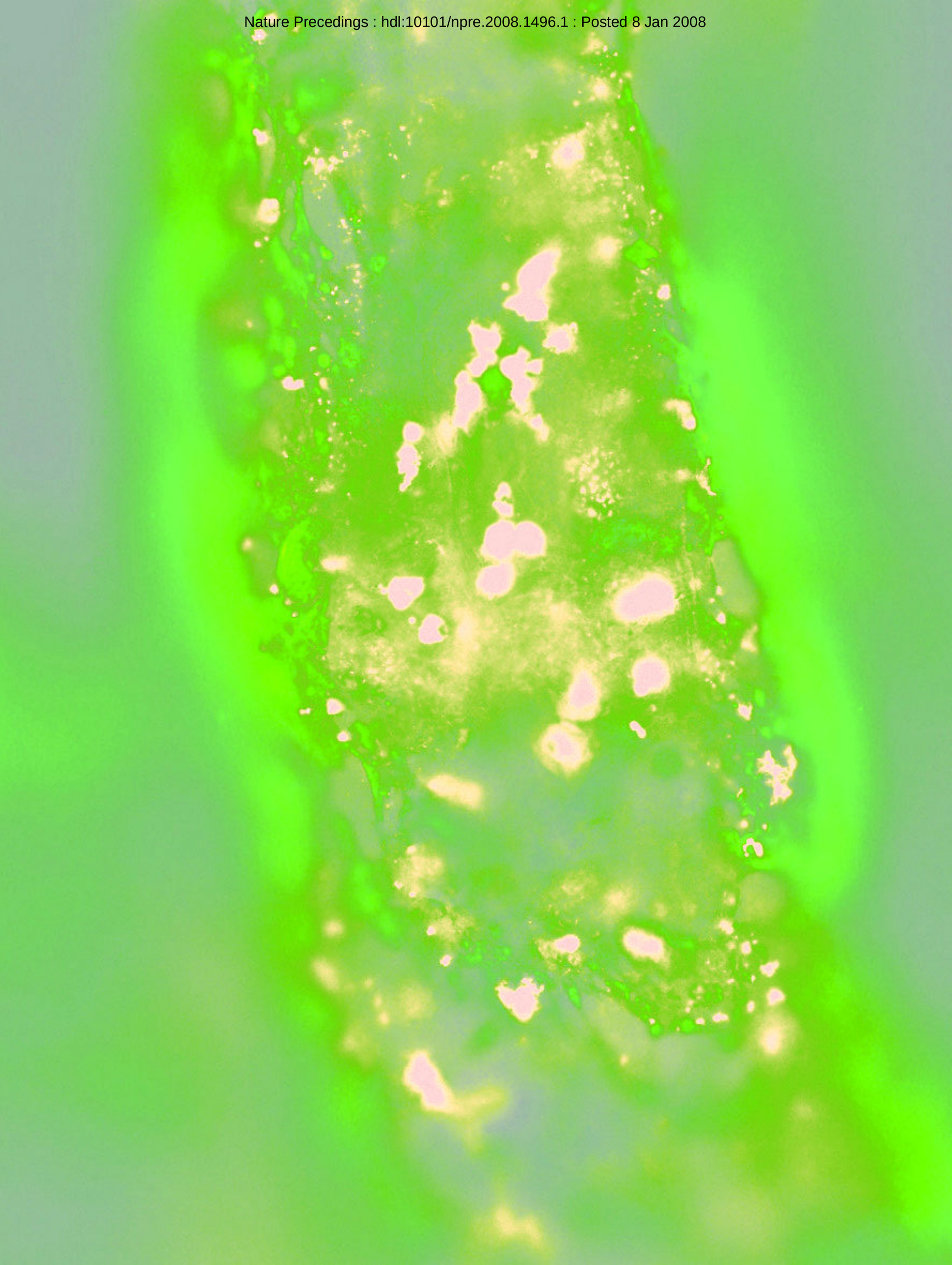

a.

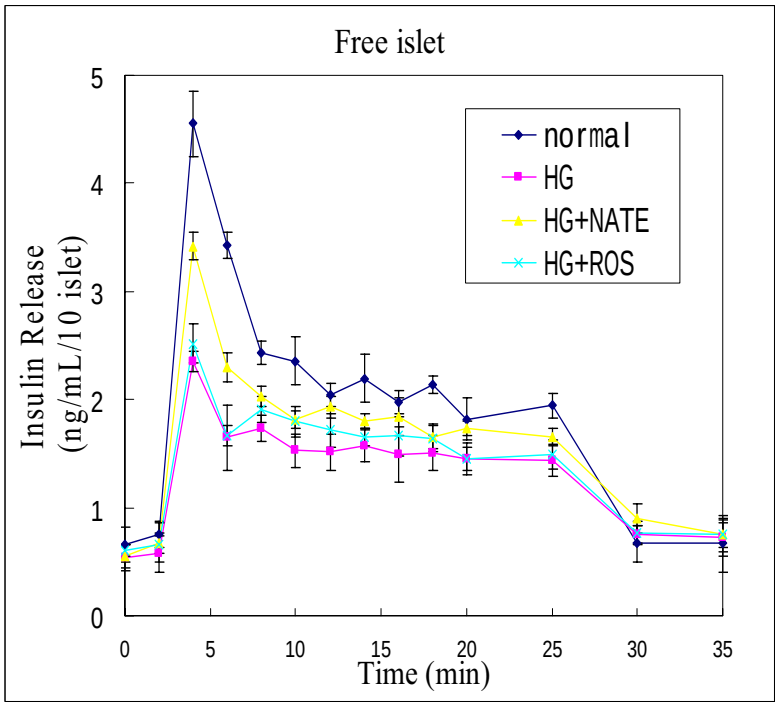

b.

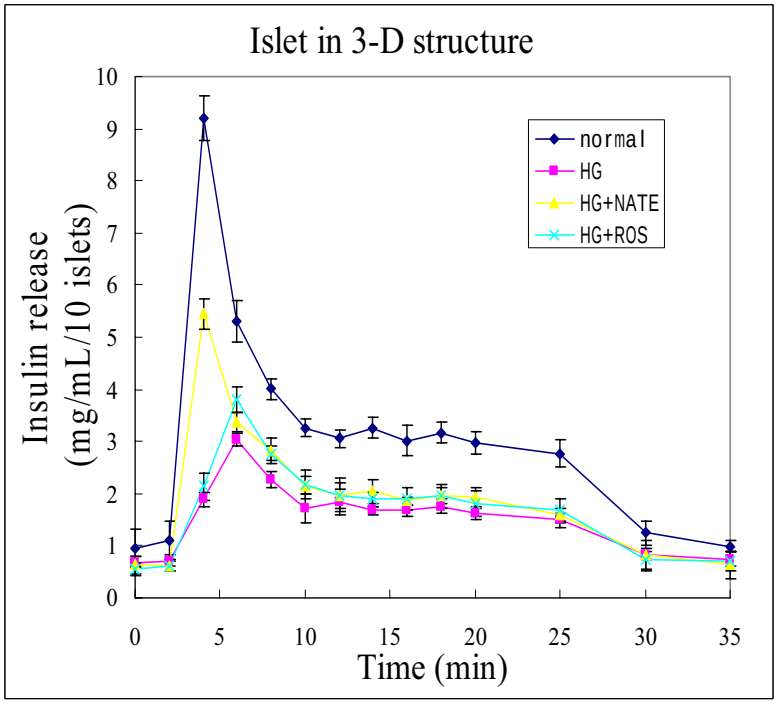

Figure 3 | Insulin secretion kinetics of **(a)** the free islet, **(b)** the islet assembled in the 3-D structure were measured by perfusion experiments. Cells were incubated in normal glucose (**NG,** 5 mM) or

high glucose (**HG**, 15 mM) for 5 d. For drug experiment, rosiglitazone (**ROS**, 3 μg/ml) or nateglinide (**NATE,** 5 μg/ml) were added to the **HG** culture medium at the 4^{th} day. Next the cells were introduced to a perfusion chamber and exposed to flowing perfusate with a basal glucose concentration (2mM) for 1h and then switched to a high glucose content (15 mM) perfusate for 20 min. Then the perfusate was returned to basal glucose concentration. The insulin content in the extracts was determined by ELISA insulin kit. Data are mean ± s.d., n=3.

a.

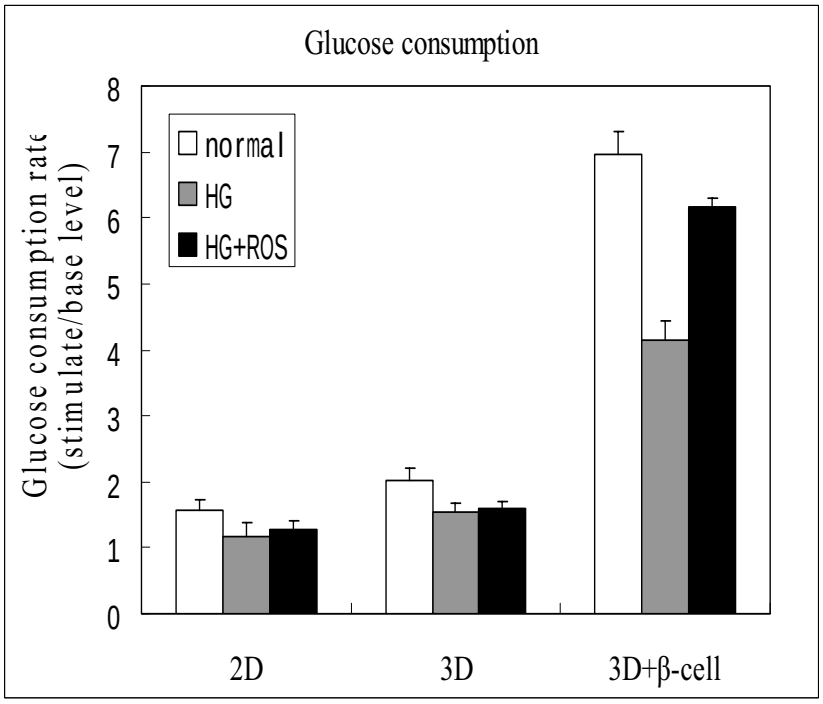

b.

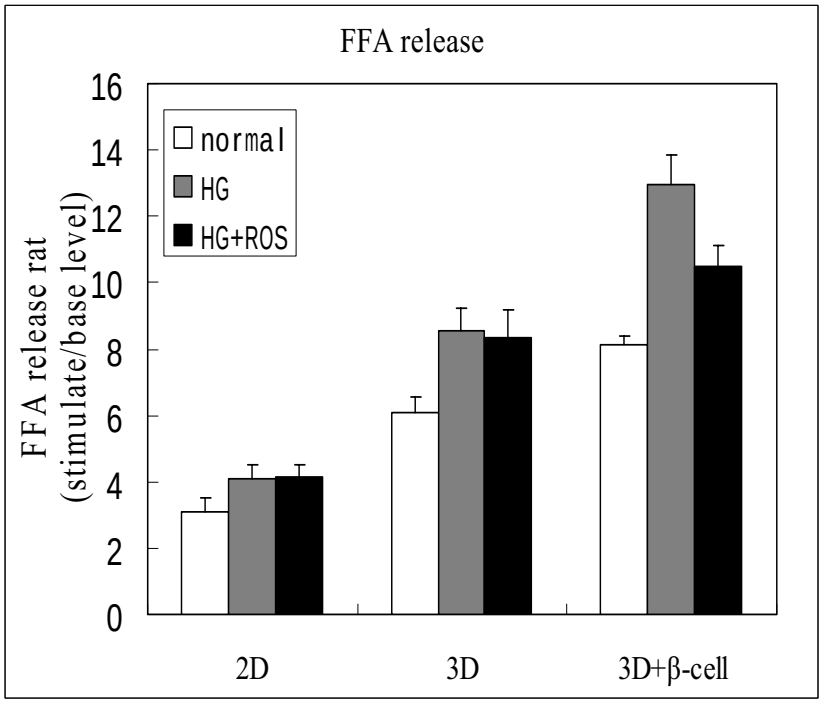

c.

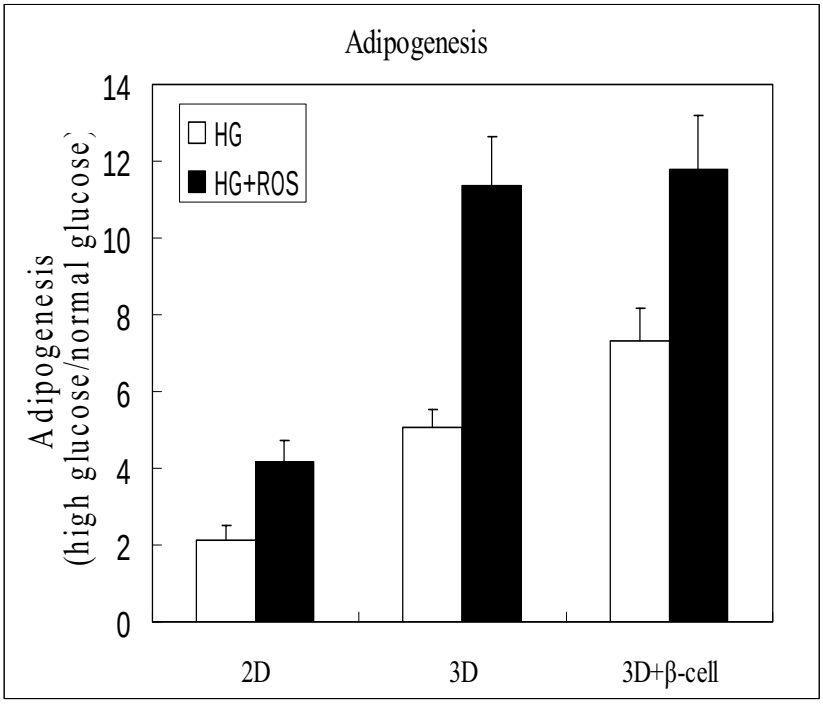

Figure 4 | Measurement of Glucose metabolism and lipid metabolism. Long-term exposure to high glucose **(HG** 15 mM**)** was used to induce the pathological changes of the cells in different culture system. For drug experiment, rosiglitazone (**ROS**, 3 μg/ml) was added to the HG culture medium. **(a)** Glucose consumption of cells was stimulated with 25 mM glucose and the glucose concentration of the medium was measured with Glucose assay kit. **(b)** FFA release of cells was stimulated with isoproterenol (10 μM) and the FFA content was measured with FFA assay kits. Results were expressed as the ratios of the stimulate level to base level. (**c**) Adipogenesis.was stimulated by long exposure to HG and the lipid accumulation was measured with oil red o assay. Absorbance is designated as 1.0 for cell cultured in normal glucose. Data are mean ± s.d., n=6.

a

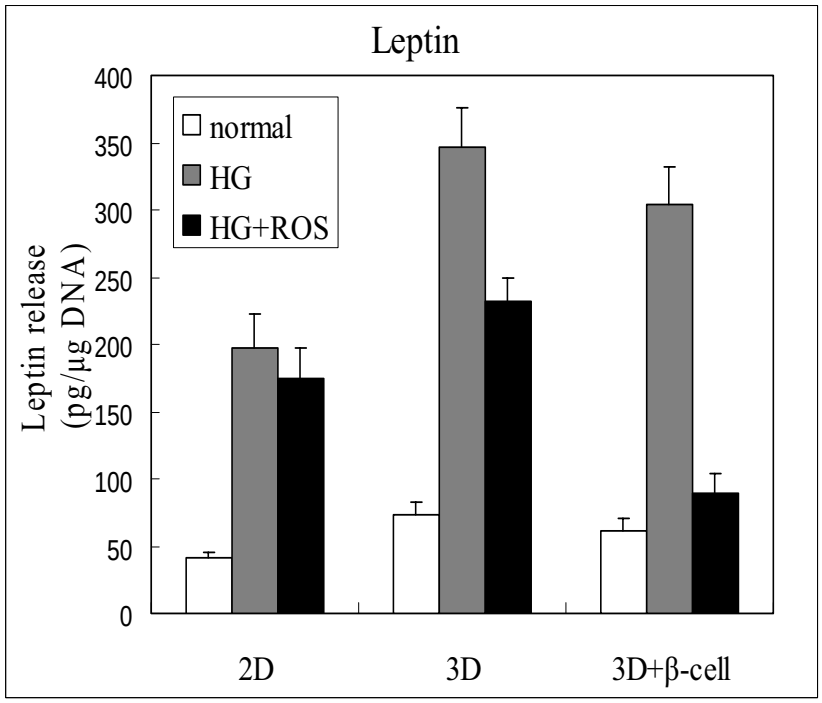

b

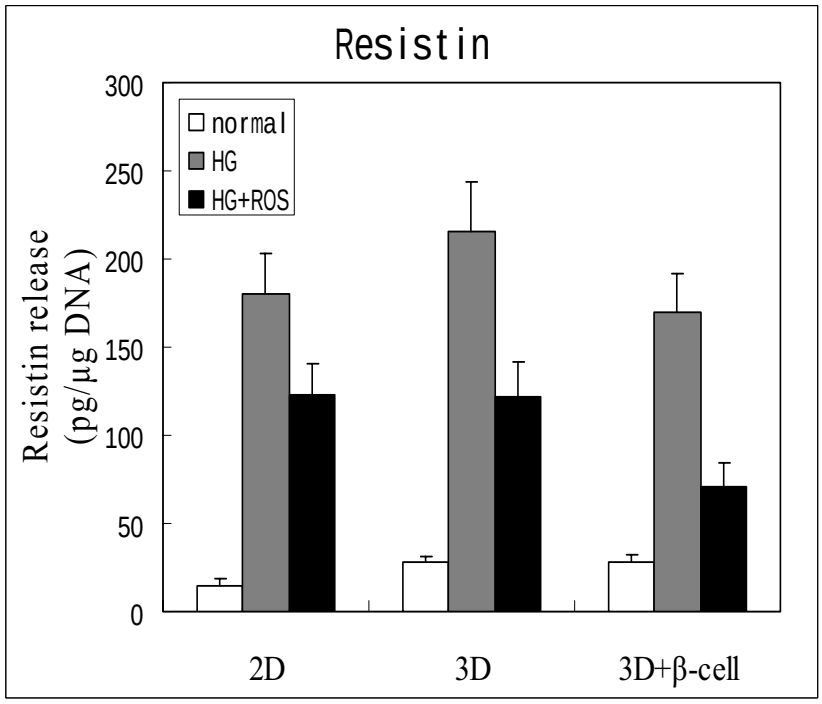

c.

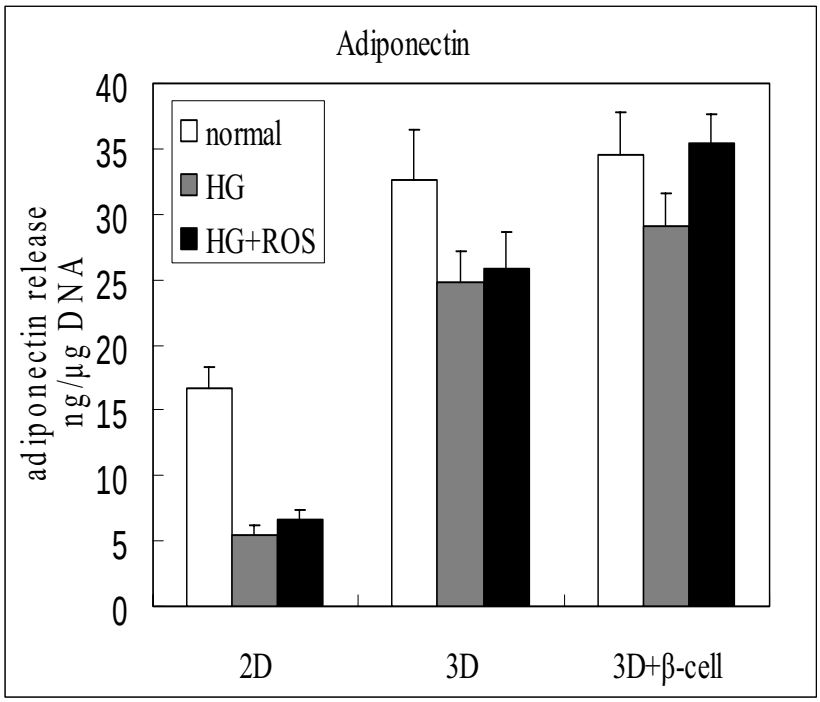

Figure 5 | Adipocytokine secretion of adipocytes in different culture systems. Long-term exposure to high glucose **(HG** 15 mM**)** was used to induce the pathological changes of the cells in different culture system. For drug experiment, rosiglitazone (**ROS**, 3 μg/ml) was added to the HG culture medium. Adipocytokine secretion of adipocytes in different culture system: (**a**) leptin secretion (**b**) resistin secretion (**c**) adiponectin secretion. Adipocytokine content in the medium was determined by ELISA kit. Results were expressed as the ratios of the adipocytokine secretion level to the DNA content of the cells. Data are mean ± s.d., n=6.

a.

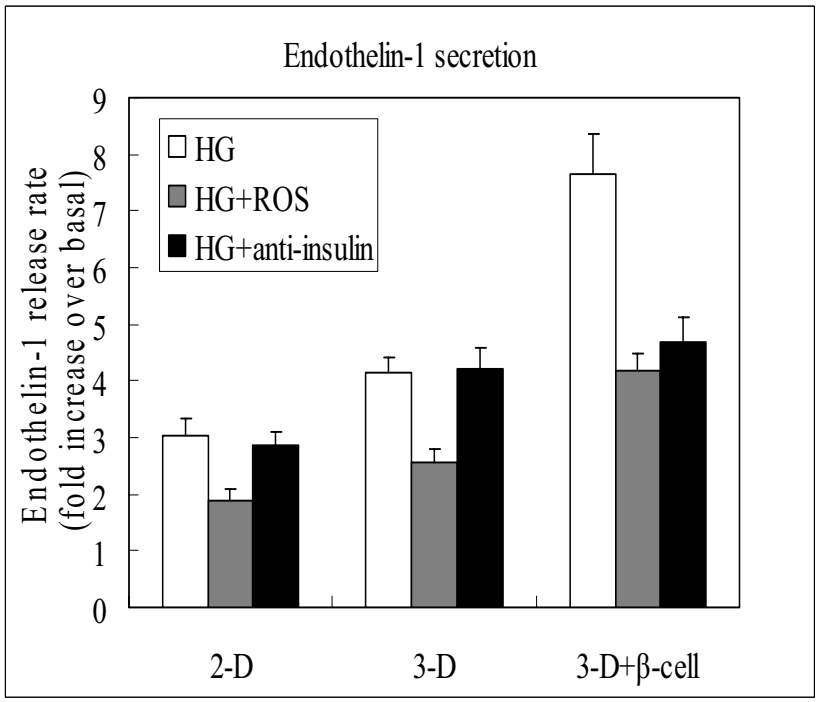

B

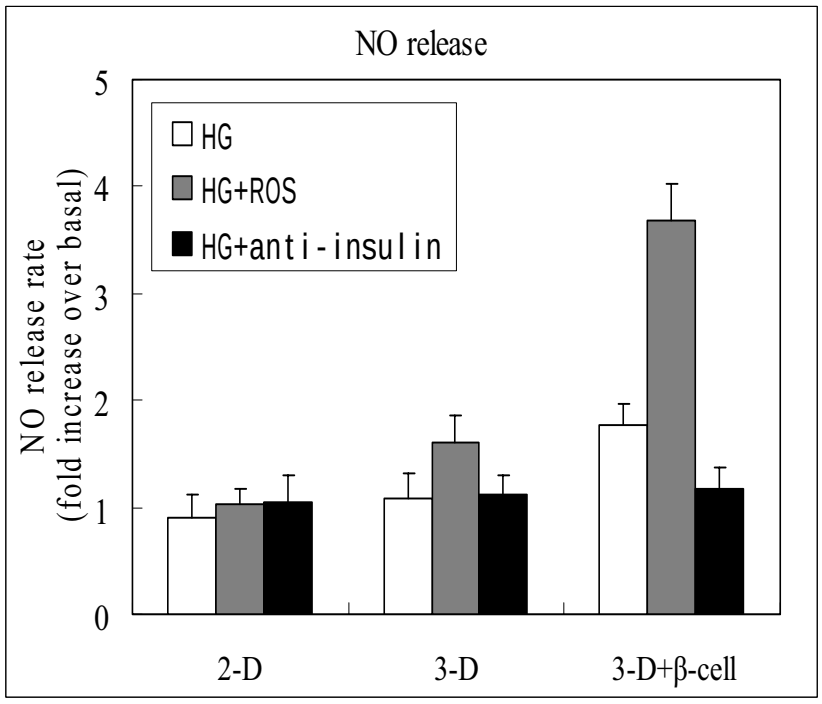

Figure 6 | Endothelin-1 and NO secretion of endothelial in different culture systems. Cells were cultured with high glucose (**HG** 25 mM) for two days. **(a)** Endothelin-1 concentrations in the

culture medium were measured by ELISA kit. **(b)** NO concentrations in the culture medium were detected by NO Detection kit. For drug experiment, rosiglitazone (3 μg/ml) was added to the HG culture medium. Results were expressed as fold increase to base level. Data are mean ± s.d., n=6.